Computational Fluid Dynamics Modeling of Scaled Hanford Double Shell Tank Mixing - CFD Modeling Sensitivity Study Results

V. Jackson
Washington River Protection Services, LLC
Richland, WA 99352
U.S. Department of Energy Contract DE-AC27-08RV14800

EDT/ECN:	DRF	UC:	N/A
Cost Center:	2GBD00	Charge Code:	200495
B&R Code:	N/A	Total Pages:	66

Key Words: WRPS, Small Scale Mixing Demonstration, SSMD, CFD Modeling, Sensitivity Report

Abstract: The primary purpose of the tank mixing and sampling demonstration program is to mitigate the technical risks associated with the ability of the Hanford tank farm delivery and certification systems to measure and deliver a uniformly mixed high-level waste (HLW) feed to the Waste Treatment and Immobilization Plant (WTP) Uniform feed to the WTP is a requirement of 24590-WTP-ICD-MG-01-019, ICD-19 – Interface Control Document for Waste Feed, although the exact definition of uniform is evolving in this context. Computational Fluid Dynamics (CFD) modeling has been used to assist in evaluating scale-up issues, study operational parameters, and predict mixing performance at full-scale..

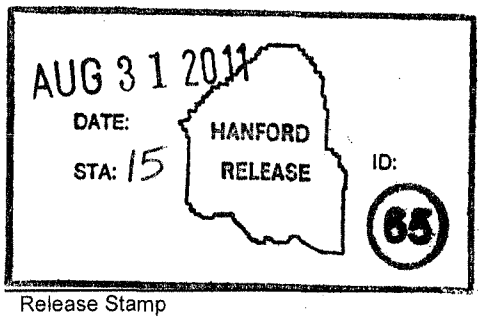

Nancy A Fonad 8/31/2011
Release Approval Date

Release Stamp

Approved For Public Release

Computational Fluid Dynamics Modeling of Scaled Hanford Double Shell Tank Mixing

CFD Modeling Sensitivity Study Results

Revision: 0
Issue Date: August, 2011

Approved By:

Dr. Wesley Bratton, Project Manager

Prepared for:

Washington River Protection Solutions
PO Box 850, MSIN H6-16
Richland, WA 99352

Prepared by:

Vista Engineering Technologies, LLC
1355 Columbia Park Trail
Richland, WA 99352

EXECUTIVE SUMMARY

The primary purpose of the tank mixing and sampling demonstration program is to mitigate the technical risks associated with the ability of the Hanford tank farm delivery and certification systems to measure and deliver a uniformly mixed high-level waste (HLW) feed to the Waste Treatment and Immobilization Plant (WTP). Uniform feed to the WTP is a requirement of 24590-WTP-ICD-MG-01-019, *ICD-19 – Interface Control Document for Waste Feed*, although the exact definition of uniform is evolving in this context. Computational Fluid Dynamics (CFD) modeling has been used to assist in evaluating scale-up issues, study operational parameters, and predict mixing performance at full-scale.

To accomplish this goal, the following three objectives for the CFD modeling were established:

1. Demonstrate that the modeled jet velocities are equivalent to the jet velocities measured in the small scale mixing demonstration (SSMD) 120-inch tank.
2. Evaluate the impact of the jet, in terms of its flow rate and rotational rate, on the mixing performance at each of the three tank scales: 43.2-inch, 120-inch, and full-scale.
3. Evaluate the correlations that occur among the various tank scales for a defined particle suspension range of 0.2 to 0.4 m/s, as well as the parameter's impacts on mixing performance.

A single full-scale CFD mesh was initially prepared to match the characteristics of Tank AY-102. From this mesh, scaled models for both of the physical models developed by the SSMD were prepared using geometrically-scaled dimensions for all the tank parameters (such as diameter and depth), as well as mixer pump nozzle diameter and locations. Therefore, the CFD models are consistent at all three scales as constructed. Details of the model are documented in RPP-48055, *Computational Fluid Dynamics Modeling of Scaled Hanford Double Shell Tank Mixing, Fiscal Year 2010 Model Development Results*. Since the model development work presented in RPP-48055, the CFD model has been adjusted using actual jet velocity measurements made in the 120-inch SSMD tank by the SSMD contractor. These measurements utilized an impellor flow meter and were used to fine-tune the turbulence parameters in the CFD model to match the jet velocities from the SSMD program. A good correlation between the measured velocities and the computed velocities was obtained and provides confidence in the model parameters.

To accomplish the objective of studying the operational parameters of mixer pump flow rate and rotation rate at the three scales (43.2-inch tank, 120-inch tank and full-scale), and their impacts on mixing performance, a test matrix of six runs was conducted using the 120-inch scale tank. The test matrix consisted of three different mixer pump flow rates and two pump rotational rates. The three flow rates for the 120-inch scaled model consisted of 58, 78, and 98 gallons per minute (GPM), which corresponds to jet velocities of 18.5, 24.9, and 31.3 ft/s respectively. The two rotational rates that were studied for the 120-inch scale model were 0.77 and 0.48 pump-head revolutions per minute (RPM). Two additional runs were also completed -- one at the 43.2-inch tank scale and other at the 900-inch (full) tank scale. These were done to verify the tank scaling theory so the results from the 120-inch runs could be translated to both the 43.2-inch scale and full-scale.

A test matrix reduction using only the 120-inch tank scale was possible since the CFD models contained only fluids, and the fluid constitutive model scales uniformly over the three scales considered. This scaling was demonstrated and confirmed using the results from a high flow rate and high rotational rate test case in each of the three tank sizes. Comparison of the results clearly shows that fluid velocities and

associated mixing performance can be simulated at all scales using the given scaling relationships and the CFD results from 120-inch tank.

Using the mixing performance results from the test matrix, the CFD results show that the pump flow rate (jet face velocity) has a larger impact on mixing performance than pump-head rotational rate within the defined particle suspension range of 0.2 to 0.4 m/s. For the 120-inch scale, changes in flow rate from 58 to 98 GPM at a constant pump-head rotational rate produced between 25 and 70% increase in the mixing iso-surface area for the defined particle suspension range of 0.2 to 0.4 m/s. Likewise a change from 0.77 RPM to 0.48 RPM in pump-head rotational rate produced changes between -20% and +6% depending on the flow rate. For the lower flow rates, it is beneficial to reduce the rotational rate to allow the jet velocity additional time to fully expand and penetrate.

Comparison across the three scales indicates that rotational rate has a slightly larger influence at the larger scales. More importantly, the areas with fluid velocities of interest related for solids suspension are relatively larger as the scale increases. This finding is partly due to the higher jet velocities utilized in the large scales, but does suggest that mixing performance and distribution of solids can be expected to improve as scales get larger as long as fluid flow is the dominant mode of solid movement. The influence of actual solid particles in these fluid-only simulation streams should be considered when predicting mixing performance.

REVISION HISTORY

Revision	Change Description
0	Initial Release

TABLE OF CONTENTS

APPENDICES

LIST OF FIGURES

LIST OF TABLES

LIST OF TERMS

ADMP	Advanced Design Mixer Pump
ALC	Air Lift Circulator
CFD	Computational Fluid Dynamics
DST	Double-shell Tank
FY-2011	Fiscal Year 2011
GPM	Gallons per Minute
HLW	High Level Waste
OTS	Off the Shelf
PJM	Pulsed-jet Mixer
Q3	Third quartile
RPM	Revolutions per Minute
SRNL	Savannah River National Laboratory
SRS	Savannah River Site
SSMD	Small-scale Mixing Demonstration
UDF	User Defined Function
V&V	Validation and Verification
Vista Engineering	Vista Engineering Technologies, LLC
WTP	Waste Treatment and Immobilization Plant

UNITS OF MEASURE

dB	Decibel
ft	Feet
in	Inch
GB	Gigabyte
GHz	Gigahertz
GPM	Gallons per Minute
m	Meters
µm	micrometers
mHz	Megahertz
mm	Millimeter
%	Percent
RPM	Revolutions per Minute
s	Second
sq. m	Square meters

1.0 INTRODUCTION

The primary purpose of the tank mixing and sampling demonstration program is to mitigate the technical risks associated with the ability of the tank farms delivery and certification systems to measure and deliver uniformly mixed, high-level waste (HLW) feed to the Waste Treatment and Immobilization Plant (WTP). Uniform feed to the WTP is a requirement of 24590-WTP-ICD-MG-01-019, *ICD-19 – Interface Control Document for Waste Feed*, although the exact definition of uniform is evolving in this context. Computational Fluid Dynamics (CFD) modeling has been used in conjunction with the small-scale mixing demonstration (SSMD) measurements to assist in evaluating scale-up issues, study operational parameters and predict mixing performance at full-scale.

One of the major reasons for conducting the CFD modeling as part of the double-shell tank (DST) mixing program was to develop scale-up relationships and full-scale predictions of the mixing performance. The CFD modeling approach is being accomplished using a graded project approach that begins fairly simply and increases in complexity with each step of the project. Prior to progressing forward on each step, a strong comparison of the CFD model results to the mixing demonstration results must occur to ensure that the model is progressing as planned and the desired project end objectives can be reached.

As demonstrated in Section 2.4 of this report, water velocities calculated within the CFD model domain along the jet centerline in the 120-inch tank scale was compared with data measured in the SSMD 120-inch tank. The model results and the measurements sufficiently match, providing confidence in the jet velocities and turbulence parameters selected for the CFD modeling. Based on sufficient water velocity matching, the next modeling step was to conduct a series of sensitivity studies to evaluate the influence of various operational parameters on the mixing behavior. This step was accomplished using three flow rates (i.e. jet velocities) and two rotational rates. All the work was conducted at the 120-inch tank scale, and scaling relationships were utilized to calculate the influences for the 43.2-inch scale and the full-scale model. Although the CFD simulations and the SSMD mixing results were not compared as described in the RPP-44619, *Computational Fluid Dynamics Modeling for Double-Shell Tank Mixing Demonstration Project Work Plan,* due to evaluation differences, the results in terms of comparisons with other tank mixing modeling scenarios are considered valid due to the internal consistencies of the comparisons.

The single-fluid CFD models have been used to facilitate understanding of mixing phenomena that occur within the tank based on the key assumption that the solid's mixing characteristics are a function of fluid velocities. Evaluation of the mixing phenomena can take many different forms, as there are various approaches to measuring and mixing performance. Given that this CFD study only considers a single fluid phase, mixing performance can only be postulated in terms of fluid velocities. Due to the complexities of the actual tank waste particle combinations, some general bounding velocity assumptions based upon previous Savannah River Site (SRS) results have been used to define a reference point of interest. The SRS results consist of a velocity of 0.3 m/s that is necessary to suspend a particle within the tank environment, as well as a velocity of 0.7 m/s to erode a pile of settled solids and mobilize that material. Based upon these SRS velocity ranges, the major focus has been upon the 0.2 to the 0.4 m/s range for the mixing performance of Hanford particles located in the tanks.

Based upon these basic constitutive assumptions, which should be confirmed or improved by the SSMD test results for Hanford-specific wastes, the CFD modeling can evaluate the scaling and performance impacts of various operational scenarios. To accomplish this evaluation, a sensitivity study using various mixer pump jet face velocities and rotational rates was established and studied using CFD models for a test matrix of six different operational scenarios. The test matrix consisted of three different jet velocities and two rotational rates. The three jet velocities for the 120-inch scaled model consisted of 58, 78, and 98 gallons per minute (GPM) flow rates which translate into jet velocities of 18.5, 24.9, and 31.3 ft/s respectively. The two rotational rates that were studied for the 120-inch scale model were 0.77 and 0.48 revolutions per minute (RPM).

The test matrix was primarily executed using the 120-inch scale model. The model only contains fluids and does not simulate particles. Since all kinematics follow the constitutive model for the fluid, all aspects of the model will scale uniformly for the characteristics affected by the assumed scaling over the size ranges considered. These constitutive relationships allow the results from the 120-inch model to be either scaled down to the 43.2-inch or scaled up to the full-scale 900-inch model. To demonstrate and validate this assumption, one CFD calculation for each of the 43.2-inch and full-scale scenarios were executed. These results are also compared to demonstrate that kinematic scaling holds.

This report presents the CFD model results from the sensitivity studies that evaluated the effects of a range of jet velocities and rotation rates of the jet nozzles. The basic premises are that the amount of mixing that occurs within the tank is related to jet's fluid velocity within the tank, which begins with jet penetration into the tank contents. As the jet velocity is increased, the distance the jet is able to penetrate into the tank contents increases. As the jet's rotational rate increases, the jet's penetration into the tank contents decreases. To evaluate the influence of these two parameters, a test matrix consisting of three jet velocities and two rotational rates was analyzed using the CFD model.

This report is structured such that Section 1.0 provides an introduction to the goals and objectives of the CFD studies that were conducted. Section 2.0 discusses the CFD model and the calibration of the turbulence parameters using a series of jet velocity measurements from the SSMD program. Section 1.0 presents the CFD iso-surface-area theory, and presents the 120-inch tank scale results. Section 4.0 recaps scaling theory and uses results from Section 3.0 to determine the scaled results for both the 43.2-inch and full-scale tank. The validity of the extrapolation of the 120-inch scale results is compared to direct simulations at the other two scales. This data is then used to examine the mixing performance results between the three tank scales. Finally, a series of project recommendations are presented in Section 5.0 and references are listed in Section 6.0.

1.1 Fiscal Year 2011 CFD Modeling Objectives

The work presented in this report is a continuation of the work conducted and documented in the RPP-48055, *Computational Fluid Dynamics Modeling of Scaled Hanford Double Shell Tank Mixing, Fiscal Year 2010 Model Development Results*. The three major objectives of this work continuation were:

1. Demonstrate that the modeled jet velocities are equivalent to the jet velocities measured in the SSMD 120-inch tank;
2. Evaluate the impact of the jet, in terms of its flow rate and rotational rate, on the mixing performance at each of the three scales -- 43.2-inch, 120-inch, and full-scale;

3. Evaluate the correlations that occur among the various scales for a defined particle suspension range of 0.2 to 0.4 m/s, as well as the parameters' impacts on mixing performance.

Each of these objectives has been addressed and is documented in this report. The CFD model turbulence parameters were tuned based upon the impellor velocity measurements conducted in the 120-inch tank. Three jet velocities and two jet rotational rates were studied at the 120-inch tank scale. The 120-inch tank was scaled using the power-per-unit-volume scaling relationship. This scaling was shown to be in agreement with the 43.2 and full-scale model runs. The mixing performance curves for a selected particle suspension velocity range of 0.2 to 0.4 m/s at each tank scale are presented to display the mixing performance. Recommendations for further development and implementation of the CFD modeling techniques are also provided.

2.0 CFD MODEL DEVELOPMENT

Advanced, commercial CFD codes are highly capable tools that are suited to a variety of unique and sophisticated problems. FLUENT®[1] is a commercial, off-the-shelf (OTS) CFD software from ANSYS®[2], that has been used to model solid suspension in both stirred and pulse-jet-mixer (PJM)-agitated tanks. The SSMD program approach will combine CFD modeling with physical testing at two scales to develop sufficient data to evaluate the tank mixing phenomena. Keeping in mind that stirring and sluicing are chaotic processes, general approximations of the actual system's behavior are appropriate. This section summarizes the model development of the single-phase velocity models only.

2.1 Hardware and Software

The CFD modeling described in this report was executed on a Dell®[3] Precision® PWS 690 64-bit computer running Microsoft®[4] Windows XP® Professional x64 Edition, Version 2003, Service Pack 2. ANSYS FLUENT 12.1 software was used for all model executions. The software and hardware system underwent a validation and verification (V&V) process that is documented, along with additional details concerning the computing system, in RPP-48055.

2.2 Model Geometry and Key Characteristics

A single full-scale CFD mesh was initially prepared. From this mesh, scaled models of both of the physical models developed by the SSMD were prepared using geometrically scaled dimensions for all the tank parameters (such as diameter and depth), as well as nozzle diameter and locations from full-scale drawings. Therefore, the models are consistent at all three scales as constructed. As-built documentation from the SSMD contractor was used for both the small-scale and the full-scale tanks. The geometry models of the full-size tank and the two scaled test beds were created separately to allow for individual deviations in the test beds. Therefore, the resulting meshes are similar in the number of computational nodes, but are not exact duplicates.

The air lift circulators (ALCs), transfer pump, and heater coil are modeled as vertical cylinders. The jet pumps are also modeled as vertical cylinders, with the nozzle faces appearing on the lower surface of the cylinder. There are 16 nozzle faces on each jet pump surface, separated by 22.5 degrees, which are coordinated to simulate a rotating pump head.

The geometric models are relatively complicated in comparison to typical fluid tanks in other industries. Legacy items such as the ALCs, heater, and many smaller features not included in the CFD model interrupt and redirect the flow path of the actual jet. Features smaller than the transfer line were not modeled.

The two physical tank sizes developed for SSMD testing are a small-scale (43.2-inch diameter) and a large-scale (120-inch diameter) tank. Since the full-scale tank has a diameter of 75 feet (900 inches), the scaling ratios for the small- and large-scale test tanks are 1/20.8 (0.048) and 1/7.5 (0.133), respectively. The key geometric features of the tanks were linearly scaled from the

[1] FLUENT is a registered trademark of ANSYS, and SAS IP, Inc., of Canonsburg, Pennsylvania.
[2] ANSYS is a registered trademark of SAS IP Inc of Canonsburg, Pennsylvania.
[3] Dell and all of its products are registered trademarks pf Dell, Inc of Plano, Texas.
[4] Microsoft products are registered trademarks of Microsoft Corporation of Redmond, Washington.

Hanford Site drawings for the AY-102 DST, to establish the design basis. The drawing references are H-2-34690: *Dome Plan Penetration Tank-102-AY*; H-2-64447: *Tank Plan and Penetration Schedule*; and H-2-34669: *Coil Assembly*. A dimensional drawing of the test apparatus provided by the SSMD contractor was reviewed to ensure that any differences between the Tank AY-102 drawings and the test platform were captured and documented for use with the CFD model. For each model, the nominal drawing values were used. Additional information on the tank geometry can be found in Section 2.2 of RPP-48055.

2.3 Boundary Conditions

Several of the boundary conditions in Hanford's DSTs are challenging (jet face parameters, suction inlet parameters, free surface boundary), and the knowledge of them is limited. Therefore, the CFD model utilizes a simplified domain, as discussed in Section 2.2 of RPP-48055. Statistically valid results were obtained by evolving the initial conditions with several rotations of the mixer jets. Starting with simple cases allowed the CFD model to be developed over time by increasing its complexity. The initial primary boundary conditions were walls and obstructions, for example.

The computational domain of the CFD model ends at the walls, where the flow transitions to laminar flow before reaching the wall – e.g. the no-slip boundary condition. The CFD model, using FLUENT, was designed to prevent laminar and turbulent flow in the same domain, since full implementation of CFD was not required, as solution of the full set of equations is an active topic in advanced research. The FLUENT program solves this issue using various known assumptions to eliminate the duality. A wall function therefore uses some experimental correlation to apply a boundary layer in the last tiny fraction of the computational cell adjacent to the wall. For this model, the standard wall function has been selected and used on the tank wall, tank floor, and ALC and heating coil obstructions until other data motivates the use of something more computationally complex.

The top of the computational domain is a free surface where fluid phases separate into air and fluid. The air in the top of the tank is not modeled, and because there is no separate phase on the bottom of the tank, the top and bottom can be modeled as walls. The stresses at the top air-fluid boundary are set to be frictionless, causing flow to approach the boundary and slide across it instead of penetrating or bouncing off it. The stress tensor at the top does not have to be zero, and in channel-flow applications, for example, a special boundary-layer function is imposed to simulate the action of the free surface. This degree of sophistication was not included at this time in the model. For now, the CFD model represents the top surface using a slip boundary condition.

In the flow domain, nozzles and intakes are surface boundaries with refined meshes. These boundary conditions are where mass, velocity vectors, turbulence, etc., appear or disappear. Flow coming into the tank from a jet nozzle that penetrates under laminar to slightly turbulent conditions will travel further into the tank than will flow with a lot of swirl, turbulent intensity, or divergent velocity vectors, which will increase the velocity's spread. For the model used in this study, a simple combination of pressure boundary outlet (jet pump "inlet"), and specified flow-velocity inlet (jet pump "outlet nozzle") is used in lieu of a more complex pump function to simulate the jet pump, which is deferred until a solid phase is added..

At this stage, with only a single-phase system being modeled, the velocity, turbulence intensity and hydraulic diameter are set at the nozzle face (pump outlet, CFD inlet), and the intake face is set to hold constant gage pressure (pump inlet, CFD outlet). Thus, mass flow in and mass flow out float a

bit. After a few time steps, mass is adequately conserved, producing reasonable results for the interior flow at low computational cost.

The average velocity over the face of the pump nozzles for each scale is taken from Table 4.2 in PL-SSMD-EG-001, RPP-44620, *Waste Feed Delivery Small Scale Mixing Demonstration Plan.* The turbulence intensity was initially 10% for each of the scales (a conservative value), and the hydraulic diameter was the nozzle diameter at each scale. Well-known correlations within FLUENT are used to obtain the two turbulence parameters (k and epsilon) on the boundary of the flow domain, using the local average velocity (which is different for each scale). This method introduces a kind of scaling such that each of the models has similar relative amounts of turbulence introduced by the pump faces. Additional work presented in Section 2.4 of this report describes the tuning adjustments made to the CFD model using the SSMD actual jet velocity measurements.

The suction return for each of the jet pumps was modeled as a uniform velocity profile across the face of the suction inlet boundary leaving the domain. The jets and suction returns were treated as boundary conditions in the bulk liquid. Therefore, mass can enter and leave the model only at these locations. Since mass is conserved, mass in will equal mass out such that mass brought out of the model domain through the pump suction inlet will equal the mass returned to the model domain through the two jets on each pump. In more complex situations, this condition is handled by a User Defined Function (UDF). In the present case, balance is achieved by a simple pressure boundary condition. For the water-only cases, only the volumetric flow rate and temperature is needed for each jet pump (i.e. pair of nozzles).

Additional detail of the modeling of the jet pumps, nozzles, and associated turbulence can be found in RPP-48055, which provides the details of the jet nozzle orientation and the modeling of the rotational aspects of the jet.

2.4 CFD Model Tuning

The CFD model was calibrated using a series of water-only velocity measurements that were made in the 120-inch SSMD tank, and not as described in RPP-44619, but as described later in this report. The actual measurements were made using a flow impeller to collect a limited dataset from only the 120-inch SSMD tank. This dataset was collected to aid in tuning and the development of theoretical models. The 120-inch tank flow velocity measurements were collected with the ALCs raised up out of the way, but not completely out of the tank.

Figure 2-1. Alignment of CFD Jet

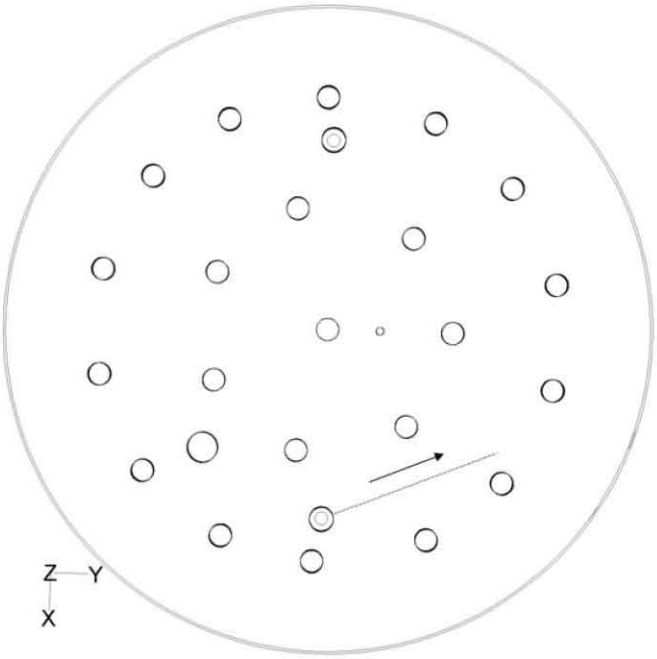

The CFD model used for comparison to the experimental results was created with the ALCs in place (and is identical to the regular 120-inch scale CFD model configured to simulate one jet pump at a fixed angle). The rotational jet angle chosen for the experimental measurements was selected such that the centerline of the jet was

oriented between ALCs, to minimize both the flow interference from the ALC's in the tank as well as the simulation (22.5 degrees counterclockwise from the y-axis). Figure 2-1 shows the alignment of the jet pump used in the CFD simulations (only the section sampled is shown, and the arrow indicates the flow direction of the jet). The DVD in Appendix A has video of the actual tank with the flow meter in operation. For the SSMD measurements, the jets rotation was held stationary, but both mixing jets (4 nozzles) were operating.

Figure 2-2. Control Rod with Bottom Foot.

The impellor flowmeter was a SWOFFER®[5] Model 3000-1514 (serial #8604). The impellor centerline was mounted 2.5 inches above the base of the foot unit (see Figure 2-2 for a photo of the impellor). The foot unit provided stability to the flow meter during velocity measurements. It allowed the flow meter's control rod to press firmly against the tank bottom. This pressure reduced the deflection of the rod that occurs due to the high velocity flow field coming out of the jet. The control rod was used to control the meter from the top of the tank. At each measurement location, the flowmeter was centered at the measurement point and then rotated to achieve the maximum velocity reading, indicating that the flow meter was generally aligned with the flow direction. These measurements were conducted at a series of locations along the centerline of the jet flow. A video of the measurement process for one location is provided on the DVD in Appendix A of this report. This video indicates the difficulty of precisely positioning the measurement device in the high flow stream immediately coming out of one of the jet nozzles.

Two volumetric flow rates were tested: 90 and 110 GPM. The 98 GPM CFD model data at the rotational angle that matched the measurements was used to compare with the average SSMD measured results from the two-flow rates after normalizing by jet velocity and nozzle diameter. The CFD model calculated the velocity along a series of vertical straight lines arranged along the centerline of the jet at various nozzle-diameter distances as show in Figure 2-1. This dataset allowed the jet to be tracked as it dropped towards the bottom of the tank (and to neutralize the impact of the non-uniform mesh along the jet). It should be noted that the CFD results are cell velocities using the existing gridding and represent an average velocity over an area much smaller than that of the impellor flow meter (the cell size opens up more towards the wall away from the pump and ALCs), which averages the velocities within the diameter of the impellor (1.975 inch). This difference in representative areas represents one of the major differences in the two measurements that must be considered as the data are compared.

The velocities in Figure 2-3 have been normalized by the average velocity at the jet face. The distance from the jet face has also been normalized by the jet diameter to create a normalized non-dimensional plot. In Figure 2-3, the dataset corresponding to the directional line identified in Figure 2-1 was used to represent the CFD calculated velocities along that line from the jet face towards the tank wall. The data points on the plots are the average normalized velocities from the SWOFFER 3100 flowmeter. Each location was measured twice. Error bars of +/- 15% have been added to the data points to suggest uncertainty in these measurements.

[5]SWOFFER is a registered trademark of Swoffer Instruments, Inc., Seattle, Washington.

The CFD calculations and measured data show good agreement away from the nozzle face. However, there are several factors that should be considered when evaluating this comparison. The physics of the measurement apparatus and devices as well as the key boundary conditions should be considered. When a turbulent jet of fluid is discharged from a nozzle into a stagnant fluid medium, it both entrains fluid and expands. The fluid domain for a large-scale tank has solid wall boundaries on the side(s) and bottom , and often internal components, e.g. ALCs and a free surface boundary on top. The jet expands into the downstream region, but then ultimately returns to the suction on the bottom of the pump, interfering with the jet in the process.

The spreading fluid is retarded by the interaction with the walls, and part of the flow that attaches to the floor after a certain distance may be expected to look like a kind of boundary layer. Entrainment of quiescent fluid and solids occurs near the outer edges of the flow, and accordingly resembles a free jet in these regions (*The Theory of Turbulent Jets*, Abramovich 1963). Most mixing action and entrainment occurs in the region of fully developed flow, which begins at a distance of about eight nozzle diameters from the exit plane (Abramovich 1963). When a turbulent jet of fluid is discharged from a nozzle with a diameter, d_o, into a quiescent fluid, the non-dimensional velocity, V_n, distribution along the jet axis for a homogeneous fluid is approximated by a constant (B) times the inverse of the non-dimensional distance x along the axis:

$$V_n = B\,(x/d_o)^{-1} \qquad EQ\ 1$$

For a free jet, the constant, B, is found in Abramovich 1963, to be 6.32. This value does not have effects from nearby walls or floors and is the solution in an infinite half space. For SRS, Tank 18, the constant (B) was found to be 4.874. This number compared well with both our data as well as the measured test data for the Advanced Design Mixer Pump (ADMP) in an 85-foot diameter tank with 70 inches of water using a six-inch nozzle diameter located 27 inches above the tank floor with a flow rate of 5,200 GPM and a nozzle velocity of 17.98 m/s ("Mixing in Large Scale Tanks - Part I - Flow Modeling of Turbulent Mixing Jets," Lee et al 2004).

For the Hanford DST mixing scenario, where the floor boundary is very near the jet centerline and the suction return is in this same region, the constant can be expected to be even lower than 4.87. The SSMD measured data raises concerns because it shows an almost linear decay that continues to decrease even at points beyond 30 nozzle diameters. According to the standard fluid dynamics theory, the decay rate at this distance should be less than it is at closer distances. Possible explanations for linear decay of the SSMD measured data include the large diameter of the impellor creating an average of the jet velocity as it tends to the tank floor and the return suction also traveling along the floor bottom. The CFD results do not show this linear decay, and better match the theoretical slope as shown in Figure 2-3.

Other factors that affect the degree of fit between the CFD results and the measured data include the location of the measurement points along the centerline. Although every attempt was made to ensure that the meter was located along the centerline of the jet, the jet itself was in a fixed positioned 2.5 inches above the tank floor and directed at an angle to reduce any ALC influence. This fact may explain some of the error because the probe may not have been positioned directly in the jet centerline flow. The video in Appendix A, showing the measurement process, clearly demonstrates that the flow is moving very swiftly out of the jet nozzles and positioning the meter in this high flow field is difficult. Although spots were marked and observed on the bottom, exact positioning of the probe in this environment was very difficult. Finally, the rotational alignment of the impellor flow meter was performed by rotating the flow meter to obtain the maximum velocity.

The flow meter may or may not align with the jet, depending on the positioning previously described. The impellor flow meter converts rotation rate to velocity with built-in software that is proprietary, and the probe was not calibrated in a channel flow prior to use. However, the factory calibration represents sufficient accuracy for these types of measurements.

The turbulence parameters, k and epsilon, in the CFD model were specified with the option to use turbulence intensity and hydraulic diameter (from the jet nozzle size). The range of turbulence intensity tested was from 1% to 10%. A typical value used in other applications, as a ballpark starting value, is 4%. Unfortunately, the turbulence in the CFD simulations was dominated by grid dispersion, so changing the turbulence intensity had limited effects. However, the decision was made not to make the grid finer just for this purpose because the current cell count was already large (the complete model was used and not refined to better define the jet shape). If the ALCs and other tank obstructions were not modeled, it is believed that a better approximation of the near pump region could have been obtained because the mesh would be more uniform near the jet pumps. This study was focused on the region beyond 20 jet-nozzle diameters, which was adequately modeled with a turbulence intensity of 10% as can be seen in Figure 2-3. In this region, a good comparison between the measured data and the CFD model results was obtained.

The nozzle functions were also modified to attempt control of grid dispersion and obtain a better fit to the measured data. The nozzle function was utilized to create better penetration of the jet by focusing the flow at a point approximately five nozzle diameters in front of the nozzle face. This affected the early portions of the curve out to a distance of approximately nine nozzle diameters. Beyond this distance, the mesh coarseness began to influence the model results, as shown by the curve dip at 15 nozzle diameters. Since the majority of the work being performed by the mixing jet within the tank is done away from the jet nozzle, refining the mesh to improve the model's representation of the early part of the curve was not considered to be extremely important. It was assumed that matching the curve at 20 nozzle diameters and beyond in a conservative manner was more important, and the matching was accomplished.

Another factor in the comparison was the different boundary conditions on which the theoretical equations and solution are based. The Hanford jet is not a true free jet as postulated in EQ 1. Fluid can be entrained behind, on top and below the jet. It is not just a boundary with fluid that must transition from static to dynamic. In addition, the suction inlet at the bottom of the jet is a major influence. The suction inlet produces fluid motion in the opposite direction to that of the jet. This motion will create additional drag on the jet as the fluid has to move against fluid moving in the opposite direction. For these reasons, the centerline velocity in the CFD models decays faster than the theoretical wall jet scenario.

Computational Fluid Dynamics, using FLUENT has met with success, fits within expectations and follows established trends. The final CFD model data agrees reasonably well with the actual measured data from the 120-inch tank, using the average 90 and 110 GPM flow rates as shown in Figure 2-3. There is room for improvement, but given the various other uncertainties, such as final design of the mixer pump and knowledge of its turbulence factors, actual jet velocity and rotational rates, the values provide sufficient confidence in the reasonableness of the CFD model results. Since the CFD results are used and compared against themselves in this report, the results are all consistent and any possible error in tuning of the turbulence parameters will be consistent across all the results.

Figure 2-3. Jet Velocity Data for the 120-Inch Tank (Velocity Matched).

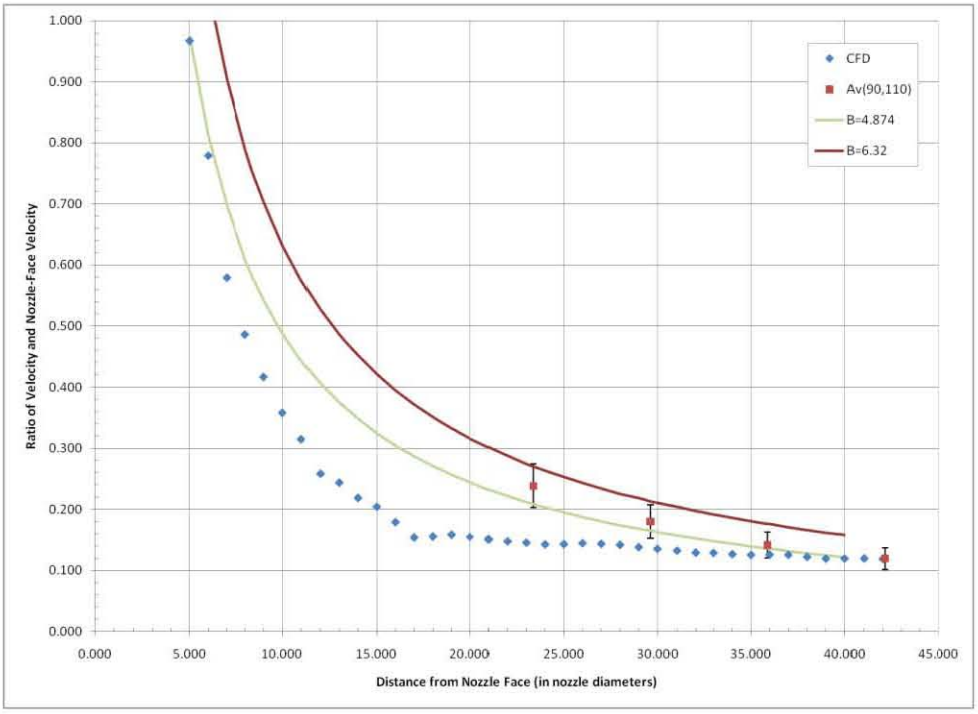

3.0 120-INCH TANK SCALE SENSITIVITY STUDIES

3.1 Introduction

A table of simulations to perform in fiscal year (FY)-2011 was provided, encompassing nine computer runs from three scaled flow rates, measured in GPM, crossed with two pump rotational speeds, measured in RPM. The completed runs are shown in Table 3-1, where seven of the nine have at least three complete rotations, and all obtained adequate statistics for analysis.

Table 3-1. Fiscal Year 2011 Simulations.

Model Name	GPM	RPM	First Restart Written	Last Restart Written	Days Elapsed	Rotations	Days per Rotation
120-Inch	98	0.77	12/13/2010 4:05	12/25/2010 8:55	12.20	4.00	3.05
120-Inch	98	0.48	12/27/2010 13:51	1/5/2011 16:06	9.09	3.11	2.92
120-Inch	78	0.48	4/11/2011 12:32	4/19/2011 5:58	7.73	3.00	2.58
120-Inch	78	0.77	4/4/2011 12:36	4/10/2011 19:54	6.30	3.00	2.10
120-Inch	58	0.77	1/19/2011 16:07	1/25/2011 2:06	5.42	3.00	1.81
120-Inch	58	0.48	1/5/2011 18:06	1/13/2011 8:44	7.61	3.33	2.29
43.2-Inch	8.6	1.51	3/23/2011 21:34	3/31/2011 8:09*	7.44	0.55	13.61
43.2-Inch	8.6	1.51	4/23/2011 3:50	4/25/2011 17:23*	2.56	0.30	8.64
Full-Scale	10400	0.2	1/27/2011 17:50	2/9/2011 21:21	13.15	3.00	4.38

Note: *Last pump index not included, stalled.

Using the current CFD model results, it has been demonstrated that FLUENT can adequately handle problems in tanks with complex internal configurations. However, each application is different, and a new approach is needed to address the specific operating conditions in question. A similar effort was conducted at SRS for the ADMP (Lee et al 2004). At SRS, a full-scale mixing pump was fabricated and tested in a partially filled, full-scale tank as described in Section 3.0 of RPP-48055. In addition to the full scale testing, a CFD model was created of the mixing pump and the resulting jet flows. The data for SRS, (Lee et al 2004) along with others, have indicated that fluid velocity, particle size, specific gravity of the particle and tank liquid level are key parameters associated with particle suspension. When erosion begins, it is dependent on the critical shear stress. The critical shear stress of the cohesive sludge materials depends on the composition of the sludge material, the particle-size distribution, particle shape and packing. A minimum fluid velocity for suspending cohesive sludge at SRS was established and confirmed as 0.7 m/s (2.27 ft/s) (Lee et al 2004). This velocity will erode the sludge layer for particle sizes larger than clay material (about 5 μ m). The velocity required to maintain such particles in suspension within the tank environment was 0.3 m/s (0.98 ft/s). Establishing these characteristic velocities for SRS sludge allowed SRS to find the local fluid velocity at any distance from the nozzle (with CFD) and use it as a measure of the capability of the jet submerged in the sludge bank to form a slurry and carry that slurry around the tank.

Estimations of minimum suspension velocity, particle-settling rate and incipient erosion velocity have been performed at Savannah River National Laboratory (SRNL) to support the use of a CFD approach to understanding this problem. (See "Analysis of Turbulent Mixing Jets in a Large Scale

Tank," Lee et al 2008, for details.) For visualization purposes, a velocity range of 0.2 to 0.4 m/s (0.66 to 1.31 ft/s) has been utilized in this project. While this value may not be precisely equivalent to velocities necessary to produce equal results with Hanford waste solids, it does provide a useful reference point to judge the relative tank performance changes that occur as varying tank conditions are modeled.

3.2 Iso-Value Surface Area

Various key parameters have been studied in this report as well as the previous report (RPP-48055) to define and evaluate mixing performance based on a power-per-unit-volume scaling approach for the jet velocities. Based on these defined jet velocities, the velocity time history at a given point (i.e. the transfer pump location) scales appropriately between the tank sizes and represents the flow and corresponding mixing performance at this point (or other points). Velocity time histories are not really good measures of mixing performance, which is characteristic of the entire tank at any given time. Taking another approach, the velocities within the tank that exceed a lower value, which is required to suspend a specific sized particle and provide transport, can also be utilized to estimate mixing performance. Since particle size was not scaled, using these same velocities in each tank, and then normalizing to the full-scale tank and surface-area unit (for the iso-surface area), improved understanding of the percentage of the tank that was being mixed at a given point in time or after several rotations of the jet pump. Considering the process, measures of the area of an iso-value surface equal to a velocity magnitude commensurate with either suspension or erosion velocities could indicate when the jets are doing the most work possible. Assuming that the iso-value surfaces are mostly potato-shaped and not extremely fragmented, the relative areas of surfaces of differing velocity magnitude can be an integral measure of system performance at the different scales. The surface areas offer the primary comparison technique that is used to compare mixing performance. An example of an iso-velocity surface is shown in Figure 3-1.

In Figure 3-1, the picture on the left-hand side is the 120-inch model and on the right-hand side is the full-scale model. The scale is in absolute velocity magnitude (not scaled), so the smaller model is energizing flow to the lower intensity and comparable velocity magnitudes are confined to the volume most directly influenced by the pump.

Figure 3-1. FS-120-vmp7-upp3-dnp1-p1to3vm.mp4.

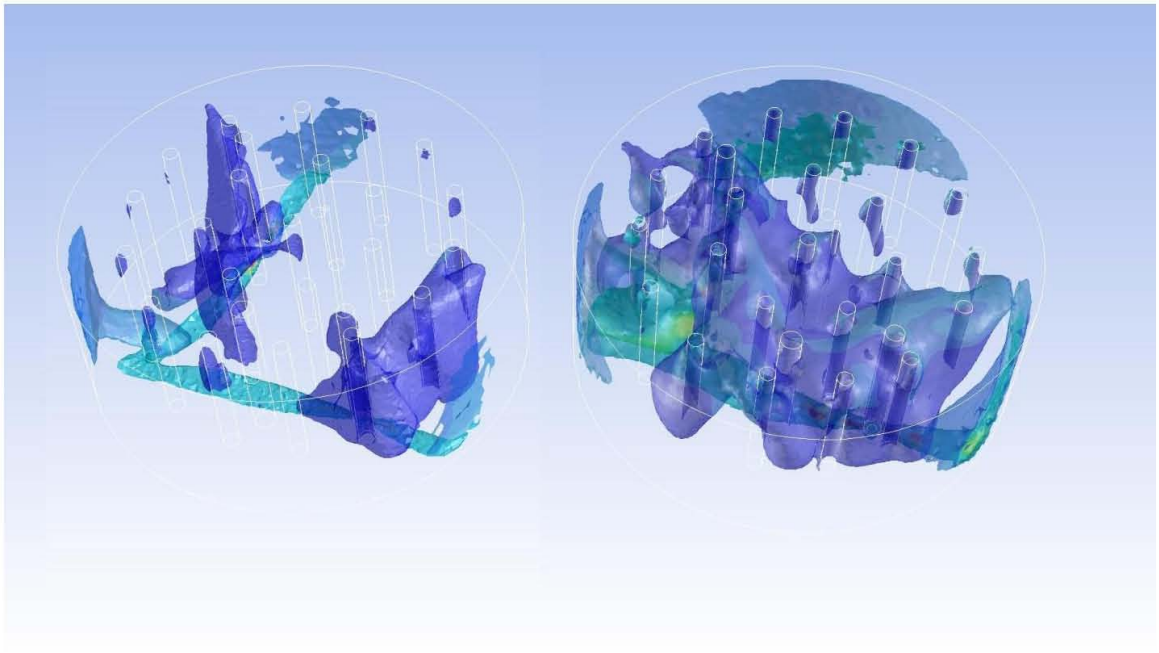

3.2.1 Statistics

Figure 3-2 shows time histories for typical iso-value velocity magnitudes during the last two full rotations of the 120-inch model. Using the last full rotations allows any variation due to start-up or flow-rate changes to settle down. By inspection, the jet-mixing process reaches a repetitive cycle as the areas fluctuate with time and jet position, and are generally steady around the mean. Quartiles, taken over a large enough time, become steady enough to use as a single value to represent the results of the simulation.

Figure 3-2. Typical Time Series for Two Full Rotations.

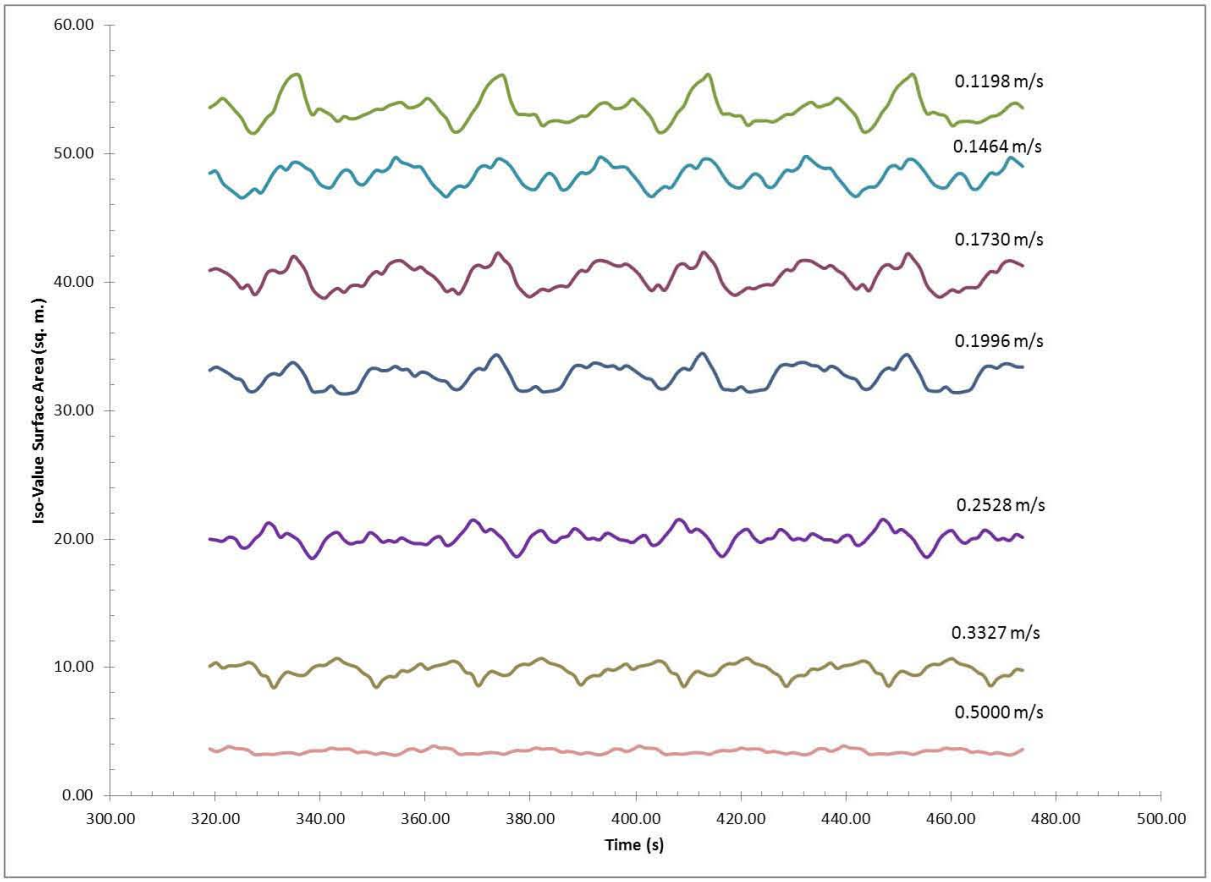

Statistical values presented in the result tables and plots were taken from the last two full rotations of the jet-mixer pumps. The only exception was for the 43.2-inch scaled simulations, where the entire range of stable values was used (repeated twice because the simulations kept stalling). A rotation of steady-state solutions at each index point of the pumps was used as an initial condition for the simulation of the 43.2-inch model. Therefore, the partial results for the 43.2-inch model are better than partial results from a cold start for collecting statistics. The normalized standard deviation of the iso-value velocity magnitude (scaled) over the time series is shown in Figure 3-3. As expected, the 43.2-inch model shows the most variation due to its limited dataset. All cases have a standard deviation below 10% over the range of 0.2 to 0.4 scaled velocity magnitudes (i.e. full-scale range mapped to the appropriate scale). This standard deviation was believed to be acceptable for comparison purposes in Section 4.2. The highest scaled velocity magnitudes showed the most variation since they surround the jets as they interact with the fluid during the pump rotation, hitting the ALCs, etc. The third quartile (Q3), as computed by Microsoft Excel, is shown in Figure 3-4 as an example. Besides Q3, the mean, Q2, is used to scale values when comparing the statistics between scales (Figure 3-3). The Q3 quartile is chosen to simplify presentation by choosing one value to plot for each simulation case.

Figure 3-3. Relative Standard Deviation All Cases (%).

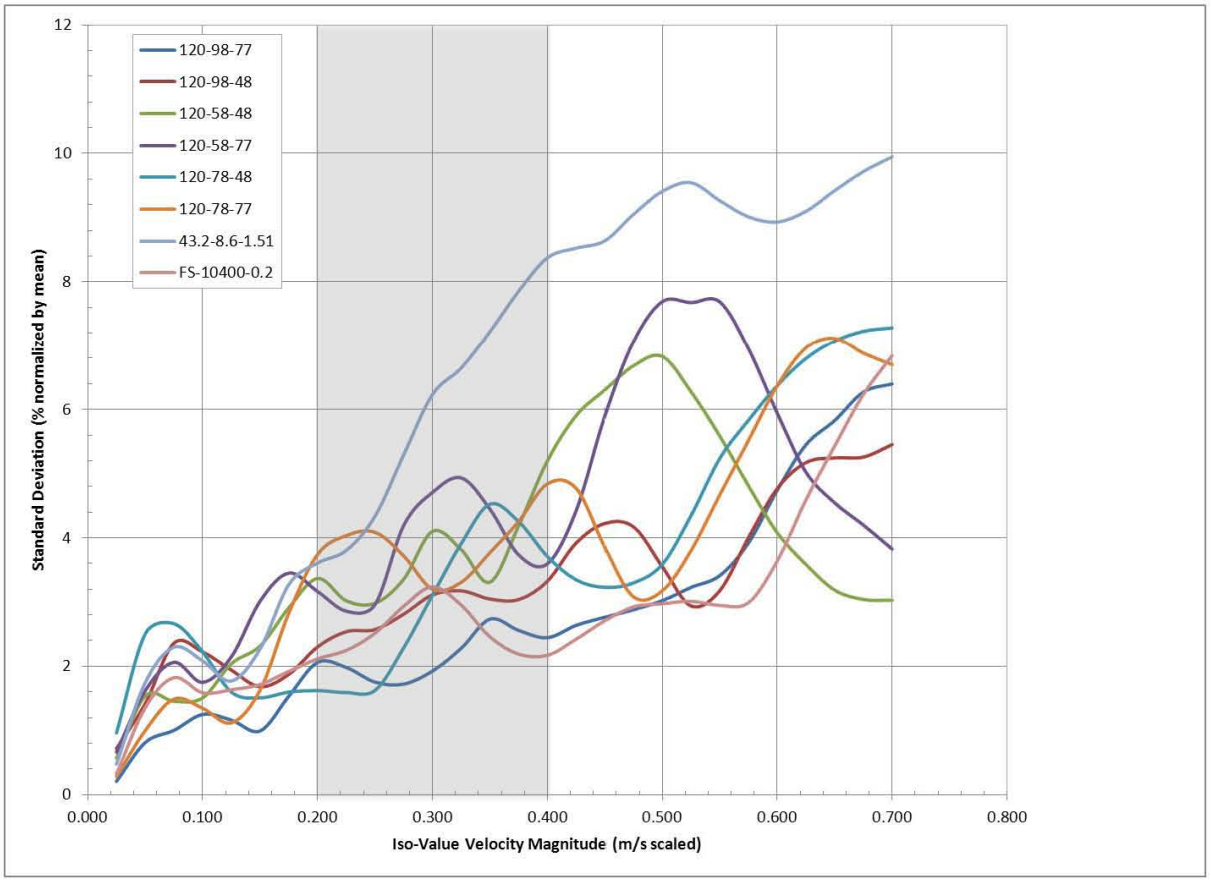

Table 3-2. Relative Standard Deviation of Iso-Value Surface Area (sq. m. and %) Versus Iso-Value Relative Magnitude (2 pages).

All Simulations

Velocity Magnitude (scaled)	120-Inch GPM=98 RPM=0.77	120-Inch GPM=98 RPM=0.48	120-Inch GPM=58 RPM=0.48	120-Inch GPM=58 RPM=0.77	120-Inch GPM=78 RPM=0.48	120-Inch GPM=78 RPM=0.77	43.2-Inch GPM=8.6 RPM=1.51	Full-Scale GPM=10400 RPM=0.2
0.0250	0.2068	0.7190	0.5683	0.6626	0.9633	0.2798	0.4766	0.3208
0.0500	0.8126	1.4194	1.5359	1.6199	2.5042	0.9979	1.7460	1.3560
0.0750	1.0016	2.3582	1.4547	2.0612	2.6621	1.4885	2.2963	1.8219
0.1000	1.2497	2.2227	1.5070	1.7489	2.2217	1.3459	2.0815	1.5861
0.1250	1.1602	1.9395	2.0398	2.1486	1.5958	1.1185	1.7700	1.6340
0.1500	0.9923	1.6804	2.3149	3.0144	1.5083	1.6278	2.2702	1.7166
0.1750	1.5355	1.8755	2.9117	3.4510	1.5976	2.8310	3.2748	1.9215
0.2000	2.0600	2.3017	3.3673	3.1632	1.6206	3.7425	3.6075	2.1156
0.2250	1.9794	2.5386	3.0195	2.8573	1.5906	4.0342	3.8037	2.2471
0.2500	1.7532	2.5713	2.9818	2.9617	1.6246	4.0854	4.3372	2.5153

Table 3-2. Relative Standard Deviation of Iso-Value Surface Area (sq. m. and %) Versus Iso-Value Relative Magnitude (2 pages).

All Simulations

Velocity Magnitude (scaled)	120-Inch GPM=98 RPM=0.77	120-Inch GPM=98 RPM=0.48	120-Inch GPM=58 RPM=0.48	120-Inch GPM=58 RPM=0.77	120-Inch GPM=78 RPM=0.48	120-Inch GPM=78 RPM=0.77	43.2-Inch GPM=8.6 RPM=1.51	Full-Scale GPM=10400 RPM=0.2
0.2750	1.7221	2.8120	3.3571	4.1947	2.2900	3.7179	5.2955	2.9355
0.3000	1.9261	3.1114	4.1013	4.7076	3.1085	3.1983	6.2334	3.2362
0.3250	2.2799	3.1737	3.8147	4.9332	3.9112	3.3076	6.6476	2.9509
0.3500	2.7347	3.0467	3.3098	4.4457	4.5239	3.7703	7.2209	2.4572
0.3750	2.5577	3.0383	4.1911	3.7334	4.2516	4.2561	7.8546	2.1882
0.4000	2.4447	3.3249	5.1996	3.5953	3.7094	4.8409	8.3734	2.1708
0.4250	2.6371	3.9202	5.9051	4.4248	3.3447	4.7697	8.5244	2.4220
0.4500	2.7627	4.2235	6.3040	5.9007	3.2280	3.8511	8.6385	2.7083
0.4750	2.8804	4.1691	6.6828	7.0665	3.2987	3.0785	9.0511	2.9249
0.5000	3.0212	3.5487	6.8274	7.6898	3.5874	3.1754	9.4091	2.9714
0.5250	3.2279	2.9388	6.2752	7.6760	4.3456	3.8009	9.5436	3.0121
0.5500	3.4119	3.1774	5.5831	7.6856	5.2372	4.6713	9.2620	2.9477
0.5750	3.9208	4.0050	4.8088	6.9468	5.8323	5.5189	9.0107	2.9904
0.6000	4.7415	4.7671	4.0791	5.9412	6.3715	6.3702	8.9311	3.6386
0.6250	5.4501	5.1717	3.5851	5.0207	6.7963	6.9624	9.0976	4.5908
0.6500	5.8269	5.2437	3.1847	4.5444	7.0714	7.1137	9.4202	5.4310
0.6750	6.2712	5.2574	3.0392	4.1973	7.2262	6.8781	9.7187	6.2362
0.7000	6.3973	5.4515	3.0269	3.8241	7.2806	6.6997	9.9461	6.8408

3.2.2 Spectra

Once the variations with time were reduced by calculating the third quartile (Q3) for the area of each iso-value surface area, a smooth curve could be calculated for each simulation run. This curve looked like an energy spectrum and behaved analogously with changes in flow rate (i.e. energy input) in the simulations. Thus, a curve of iso-value surface area versus iso-value velocity magnitude is referred to as a spectrum (plural spectra) in the remainder of the report. However, this descriptive explanation of the spectra curves is only an analogy. See Figure 3-4 for an example.

The shape of this curve approximately represents the energy dissipated by the jet-mixing process. Higher jet velocities and flow rates will change the peak location and magnitude. This excess energy will spread out over the spectrum represented by the curve. Changes in rotational rate also change the peak, but in the region of interest (shaded section) changes in flow rate are more significant as most of the rotational effect happens at lower velocity magnitudes.

Changes in rotation rate will also shift the location where the energy is dissipated. The effect is probably only significant at lower velocities, as can be seen in the sensitivity studies of the 120-inch

model shown in Figure 3-4. The small changes in rotational rate do not significantly affect the tracking of high-velocity tails of the spectra against each other. Changing the rotation rate does not affect the iso-area peak height within the velocity range of interest. For the 78 and 98 GPM cases, the high RPM (0.77) produces the highest peak iso-area, whereas the 58 GPM has the highest iso-area peak at 0.48 RPM. These GPM rates are all at a velocity below the region of interest. Table 3-3 lists the data used in Figure 3-4.

Figure 3-4. All 120-Inch Cases.

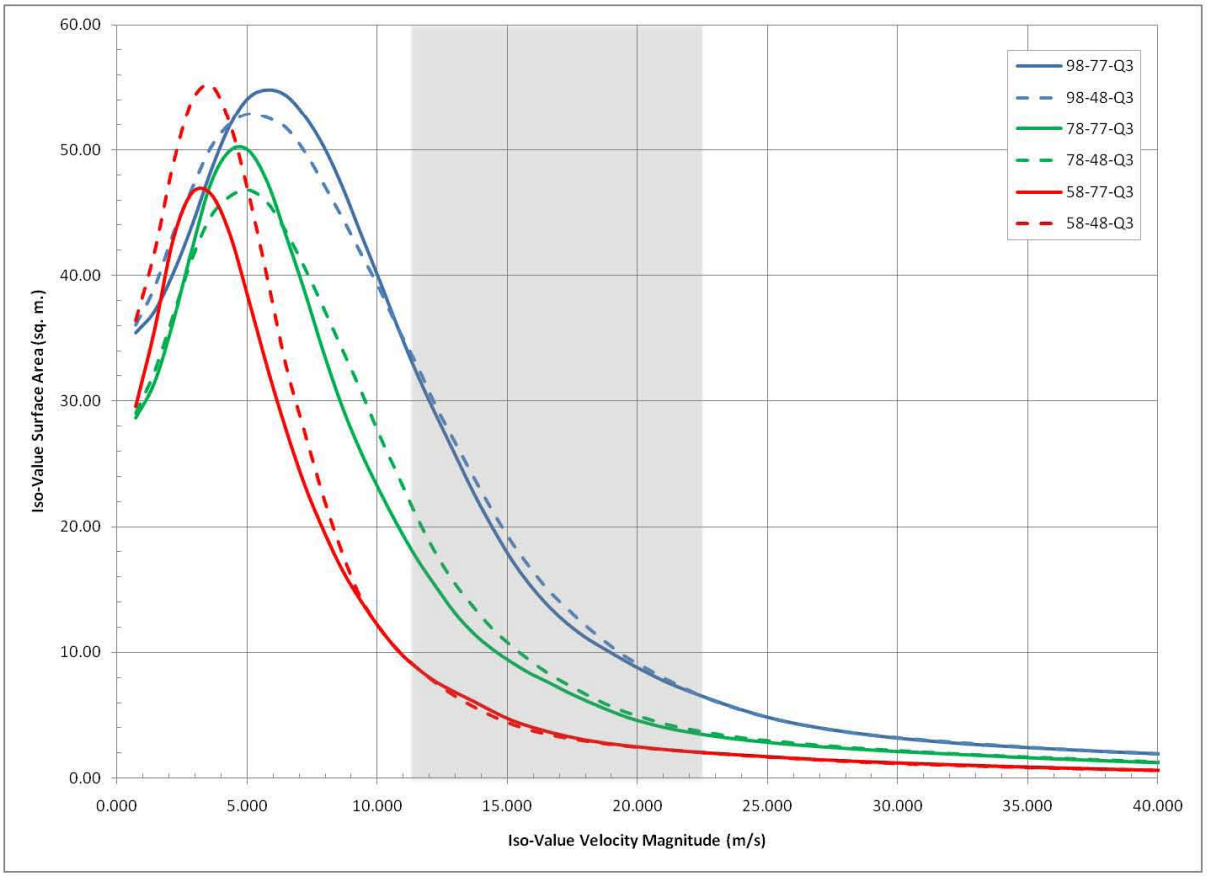

Table 3-3. Iso-Value Surface Area versus Velocity Magnitude (2 pages).

All 120-Inch Runs

Velocity Magnitude (m/s)	120-Inch GPM=98 RPM=0.77Q3 (sq. m.)	120-Inch GPM=98 RPM=0.48Q3 (sq. m.)	120-Inch GPM=78 RPM=0.77Q3 (sq. m.)	120-Inch GPM=78 RPM=0.48Q3 (sq. m.)	120-Inch GPM=58 RPM=0.77Q3 (sq. m.)	120-Inch GPM=58 RPM=0.48Q3 (sq. m.)
0.013	35.449	36.066	28.649	29.031	29.554	36.433
0.026	37.163	39.033	31.460	32.321	35.618	41.863
0.038	40.203	43.317	36.330	36.820	42.857	48.907
0.051	43.999	46.913	42.085	41.305	46.539	53.962
0.064	48.316	50.174	47.317	44.667	46.459	55.237
0.077	51.945	52.078	49.894	46.268	43.325	52.210
0.089	54.193	52.887	49.950	46.789	38.146	46.631
0.102	54.845	52.583	47.466	45.796	32.706	39.891
0.115	54.409	51.783	43.194	43.500	27.752	32.914
0.128	52.747	49.868	38.721	40.601	23.316	27.554
0.140	50.341	47.291	33.898	37.410	19.712	22.399
0.153	47.126	44.604	29.551	34.108	16.569	17.959
0.166	43.324	41.742	25.930	30.795	14.085	14.318
0.179	39.588	38.877	22.814	27.220	11.917	11.949
0.191	35.738	35.723	19.969	23.985	10.100	10.148
0.204	32.138	32.810	17.399	20.697	8.735	8.781
0.217	28.902	29.582	15.213	17.833	7.661	7.586
0.230	25.801	26.758	13.141	15.475	6.846	6.549
0.242	22.710	23.955	11.508	13.580	6.112	5.699
0.255	19.961	21.281	10.250	11.872	5.325	4.956
0.268	17.453	18.839	9.227	10.524	4.620	4.335
0.281	15.384	16.770	8.327	9.349	4.108	3.840
0.294	13.677	14.934	7.598	8.292	3.678	3.478
0.306	12.284	13.473	6.825	7.434	3.322	3.195
0.319	11.165	12.100	6.138	6.634	3.022	2.966
0.332	10.261	10.877	5.507	5.905	2.793	2.758
0.345	9.387	9.758	4.924	5.292	2.612	2.588
0.357	8.585	8.906	4.460	4.817	2.450	2.440
0.375	7.572	7.788	3.947	4.215	2.256	2.263
0.400	6.425	6.415	3.427	3.628	2.021	2.044
0.425	5.425	5.394	3.041	3.181	1.831	1.831
0.450	4.616	4.626	2.740	2.875	1.655	1.653
0.475	4.050	4.042	2.512	2.618	1.491	1.483

Table 3-3. Iso-Value Surface Area versus Velocity Magnitude (2 pages).

All 120-Inch Runs

Velocity Magnitude (m/s)	120-Inch GPM=98 RPM=0.77Q3 (sq. m.)	120-Inch GPM=98 RPM=0.48Q3 (sq. m.)	120-Inch GPM=78 RPM=0.77Q3 (sq. m.)	120-Inch GPM=78 RPM=0.48Q3 (sq. m.)	120-Inch GPM=58 RPM=0.77Q3 (sq. m.)	120-Inch GPM=58 RPM=0.48Q3 (sq. m.)
0.500	3.606	3.595	2.314	2.393	1.353	1.331
0.525	3.245	3.283	2.142	2.206	1.232	1.211
0.550	2.975	3.032	1.997	2.035	1.130	1.103
0.575	2.736	2.815	1.856	1.884	1.037	1.019
0.600	2.559	2.608	1.714	1.750	0.946	0.927
0.625	2.385	2.423	1.576	1.628	0.860	0.851
0.650	2.240	2.260	1.463	1.513	0.782	0.782
0.675	2.094	2.116	1.349	1.404	0.708	0.717
0.700	1.966	1.980	1.250	1.306	0.642	0.656
0.725	1.844	1.853	1.164	1.223	0.579	0.596

Plots of the scaled iso-value area versus scaled velocity magnitude are used in Section 4.2 to show that a single peak of approximately the same magnitude is obtained for all three scales. The peak is located further left (smaller velocity magnitudes) as the size of the model decreases. The sharpness of the peak increases for the smaller scales as well. The iso-value areas for the smaller scales are divided by the square of the appropriate geometric scale factor so that all scales can be shown together on one plot for comparison purposes.

Figure 3-5 shows the effect of shifting the iso-value velocity magnitude mapping when the 120-inch model is scaled to full-scale. The shape change is not apparent until the curves are plotted with both axes scaled. The location of the peak moves counter to the shift in the x-axis—i.e. mapping the full-scale values to smaller values at the 120-inch scale causes the peak to shift right (toward higher full-scale iso-value velocity magnitudes). The far-left spectrum (green – 120-Hi-Hi Q3) is the matching curve used in the comparison shown in Figure 4-1 and Figure 4-2. The other two spectra represent ad-hoc shifts of 0.9590 and 0.8663 relative to the normal scaling (in other words, a different mapping of iso-value velocity magnitudes from full-scale to 120-inch scale) as these FLUENT edits were available for use. These factors were chosen arbitrarily and are used only for discussion purposes.

The shift shown in Figure 3-5 shows the importance of correcting for as-is velocity variation when performing simulations and model testing. If the scaling is not exactly right for a particular set of conditions, it can be adjusted by changing the mapping of iso-value velocity magnitudes and rerunning the edit rather than rerunning the simulation or test. Values for Figure 3-5 are listed in Table 3-4.

Figure 3-5. Phase Shift with Ad-Hoc 0.9590 and 0.8663 Factors.

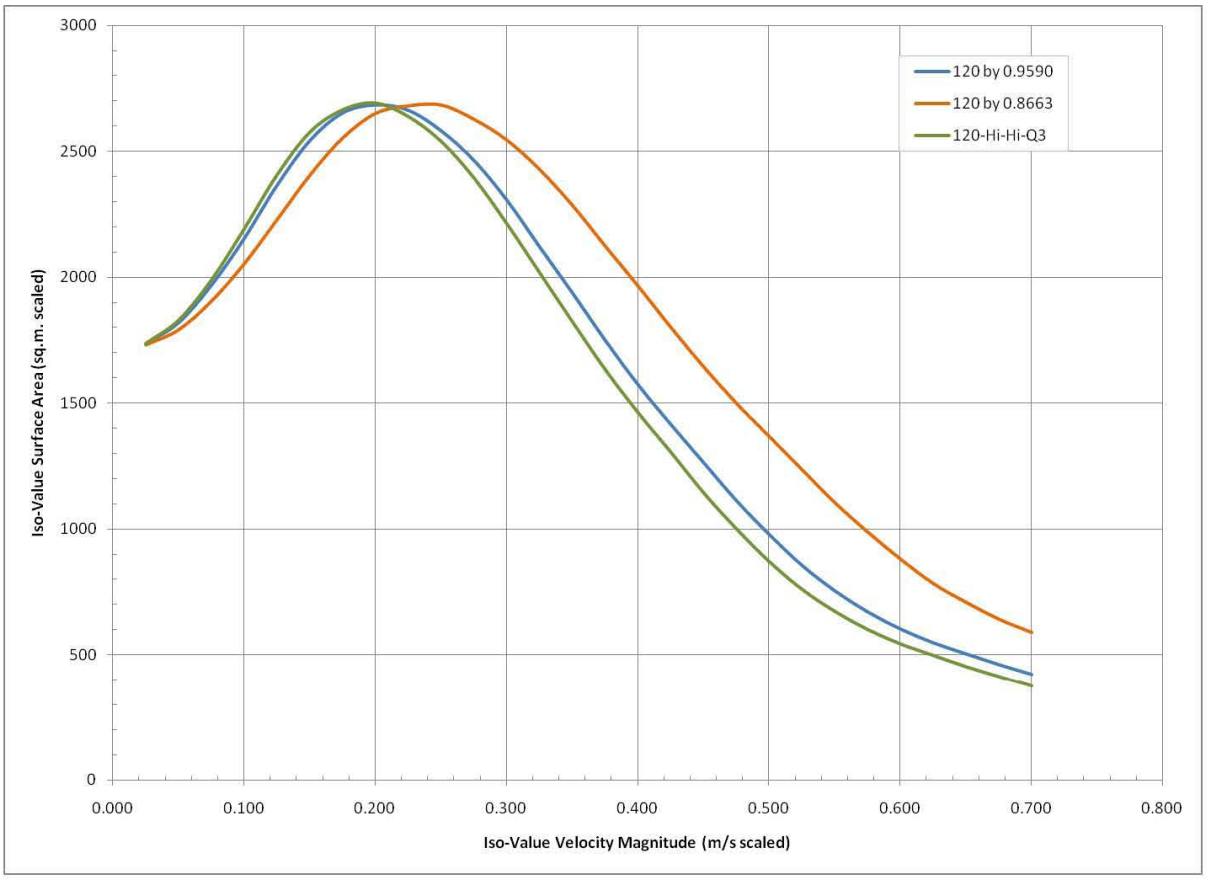

Table 3-4. Iso-Value Surface Area (scaled) versus Velocity Magnitude (scaled) (2 pages).

Phase Shift in 120-Inch Simulations GPM=98 RPM=0.77 Q3 (sq. m.)

Velocity Magnitude (m/s)	Actual Velocity Magnitude Mapping	Mapping Shifted 0.9590	Mapping Shifted 0.8663
0.025	1738.17	1736.08	1730.08
0.050	1830.80	1820.01	1789.99
0.075	1990.33	1968.88	1903.89
0.100	2193.37	2154.79	2052.41
0.125	2407.49	2366.20	2227.10
0.150	2576.89	2543.96	2403.88
0.175	2666.18	2654.03	2551.68
0.200	2692.52	2685.96	2649.35
0.225	2639.10	2664.63	2679.51
0.250	2540.59	2583.21	2682.81
0.275	2395.46	2465.37	2626.09
0.300	2214.42	2307.94	2544.09

Table 3-4. Iso-Value Surface Area (scaled) versus Velocity Magnitude (scaled) (2 pages).

Phase Shift in 120-Inch Simulations GPM=98 RPM=0.77 Q3 (sq. m.)

Velocity Magnitude (m/s)	Actual Velocity Magnitude Mapping	Mapping Shifted 0.9590	Mapping Shifted 0.8663
0.325	2019.66	2121.74	2427.09
0.350	1824.75	1938.76	2284.69
0.375	1635.10	1750.21	2122.89
0.400	1463.80	1573.93	1964.52
0.425	1306.91	1415.46	1800.23
0.450	1145.59	1263.60	1643.30
0.475	1002.21	1112.22	1498.06
0.500	872.48	977.56	1366.93
0.525	762.02	854.74	1234.70
0.550	674.35	753.44	1103.47
0.575	602.60	669.80	987.39
0.600	545.41	601.59	879.42
0.625	499.48	546.79	782.47
0.650	454.63	502.51	707.84
0.675	414.62	459.74	640.81
0.700	376.80	420.44	587.96

3.3 120-Inch Comparisons

Plots of energy-analog spectra are used to compare variations in flow rate and rotation rate for the 120-inch scale at absolute values of iso-value velocity magnitude (0.0 to 0.7 m/s).

Figure 3-4 represents the energy dissipated by the jet-mixing process for all of the 120-inch scale simulations. Higher jet velocities and flow rates change the peak location and magnitude. The increase in energy associated with higher flow rates spreads out over the spectrum represented by the curve.

Changes in rotational rate will also shift where the energy is dissipated, but the effect is only significant at lower energies, as can be seen in Figure 3-4. The small changes in rotation rate do not significantly affect how the high-energy tails of the spectra overlap in the area of interest, as shown by the sections of the curves in the shaded region of Figure 3-4.

3.3.1 Effect of Changes in Flow Rate

Inspection of Figure 3-6 demonstrates the effect of changing the pumping rate of the jet-mixer pumps. Figure 3-6 compares the percent difference between pairs of simulations at the same rotational rate. The legend of the figure indicates the flow rate and rotational rate values (GPM1, GPM2: RPM). In the key region of interest, 0.2 to 0.4 m/s, all of the curves are relatively flat and do not change dramatically, indicating that the mixing is relatively (but not in absolute terms)

constant over this velocity range. For all cases the solid and dashed lines (i.e. differences in rotational rate) track relatively closely to each other, indicating that the rotational effect is minimal in this range. Past about 0.4 m/s the absolute values of the iso-value surface areas become very small, so these percent changes are insignificant to the process. It is important to note that percent-change can be the same for both small and large absolute changes. Refer to the spectra plots for an indication of the magnitude changes. Note the smaller impact from rotation rate (maximum of 20%) as compared to the larger impact from flow rate (approaching 80%). The data used in Figure 3-6 are listed in Table 3-5.

Figure 3-6. Comparison of 120-Inch Cases at Constant RPM.

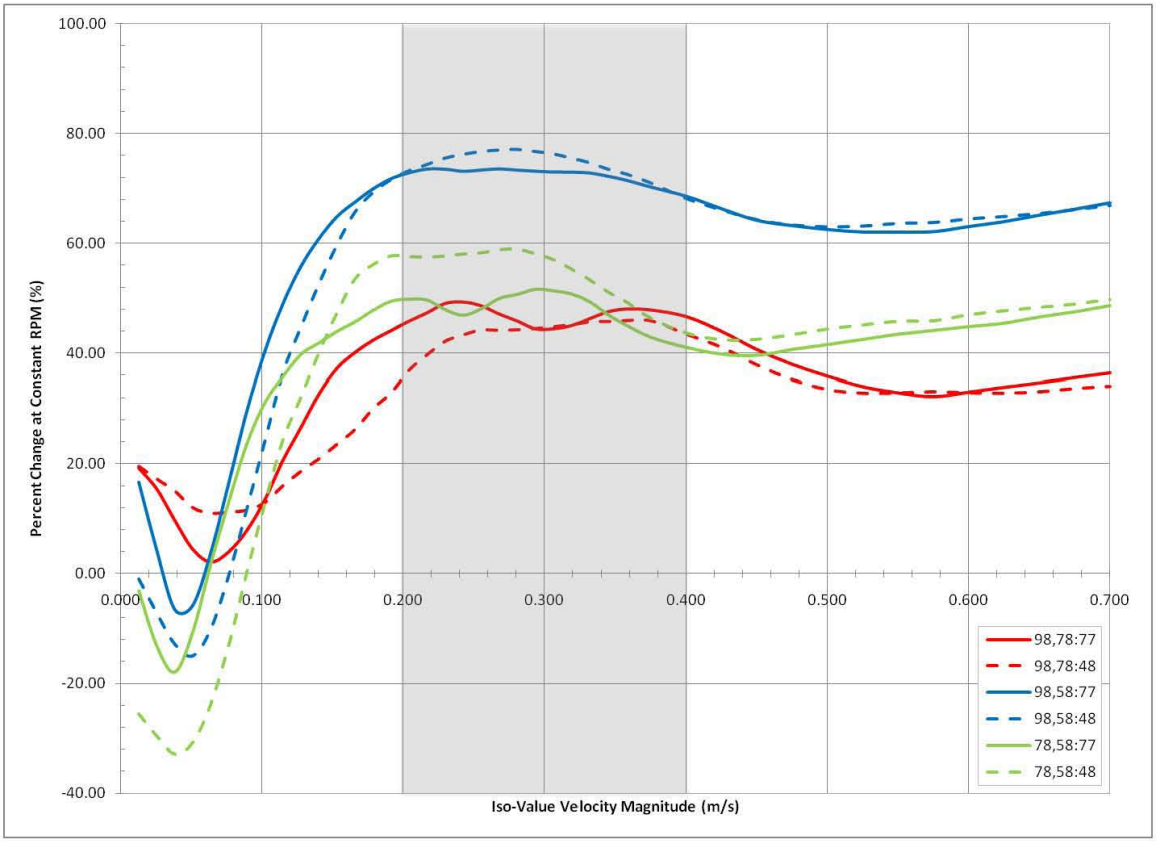

Table 3-5. Percent Change between Comparison Cases, Constant RPM (%) (2 pages).

Calculated from Iso-Value Surface Areas as 100(First-GPM - Second-GPM)/First-GPM*

Velocity Magnitude (m/s)	120-Inch GPM=98, GPM=78 at RPM=0.77 (%)	120-Inch GPM=98, GPM=58 at RPM=0.77 (%)	120-Inch GPM=98, GPM=78 at RPM=0.48 (%)	120-Inch GPM=98, GPM=58 at RPM=0.48 (%)	120-Inch GPM=78, GPM=58 at RPM=0.77 (%)	120-Inch GPM=78, GPM=58 at RPM=0.48 (%)
0.013	19.183	16.629	19.508	-1.018	-3.161	-25.499
0.026	15.345	4.157	17.196	-7.249	-13.216	-29.522
0.038	9.633	-6.602	14.999	-12.906	-17.965	-32.829
0.051	4.349	-5.773	11.955	-15.026	-10.583	-30.645
0.064	2.067	3.842	10.976	-10.092	1.812	-23.666
0.077	3.948	16.594	11.156	-0.254	13.166	-12.843
0.089	7.830	29.610	11.531	11.830	23.631	0.337
0.102	13.453	40.366	12.907	24.138	31.097	12.896
0.115	20.612	48.994	15.995	36.438	35.751	24.335
0.128	26.591	55.796	18.583	44.747	39.784	32.136
0.140	32.663	60.842	20.895	52.636	41.848	40.125
0.153	37.293	64.841	23.532	59.737	43.932	47.347
0.166	40.148	67.490	26.224	65.699	45.682	53.506
0.179	42.372	69.896	29.985	69.266	47.762	56.104
0.191	44.123	71.740	32.860	71.594	49.424	57.691
0.204	45.862	72.820	36.920	73.238	49.795	57.574
0.217	47.366	73.493	39.717	74.356	49.639	57.461
0.230	49.071	73.467	42.167	75.524	47.902	57.678
0.242	49.328	73.087	43.311	76.208	46.888	58.031
0.255	48.651	73.323	44.216	76.712	48.048	58.254
0.268	47.130	73.529	44.139	76.992	49.932	58.811
0.281	45.874	73.300	44.253	77.105	50.671	58.930
0.294	44.446	73.106	44.477	76.713	51.590	58.059
0.306	44.436	72.956	44.823	76.286	51.329	57.022
0.319	45.026	72.929	45.173	75.489	50.757	55.293
0.332	46.328	72.775	45.713	74.640	49.275	53.285
0.345	47.552	72.180	45.764	73.481	46.958	51.104
0.357	48.047	71.460	45.919	72.603	45.066	49.341
0.375	47.871	70.209	45.875	70.948	42.852	46.325
0.400	46.659	68.539	43.449	68.131	41.019	43.647
0.425	43.957	66.260	41.040	66.064	39.797	42.443
0.450	40.654	64.148	37.849	64.272	39.589	42.514
0.475	37.975	63.196	35.227	63.309	40.663	43.355

Table 3-5. Percent Change between Comparison Cases, Constant RPM (%) (2 pages).

Calculated from Iso-Value Surface Areas as 100(First-GPM - Second-GPM)/First-GPM*

Velocity Magnitude (m/s)	120-Inch GPM=98, GPM=78 at RPM=0.77 (%)	120-Inch GPM=98, GPM=58 at RPM=0.77 (%)	120-Inch GPM=98, GPM=78 at RPM=0.48 (%)	120-Inch GPM=98, GPM=58 at RPM=0.48 (%)	120-Inch GPM=78, GPM=58 at RPM=0.77 (%)	120-Inch GPM=78, GPM=58 at RPM=0.48 (%)
0.500	35.840	62.491	33.447	62.985	41.538	44.383
0.525	33.984	62.029	32.811	63.130	42.482	45.124
0.550	32.878	62.027	32.883	63.619	43.427	45.794
0.575	32.180	62.091	33.079	63.779	44.104	45.875
0.600	33.013	63.033	32.896	64.434	44.814	46.999
0.625	33.895	63.926	32.819	64.877	45.430	47.718
0.650	34.689	65.105	33.061	65.411	46.570	48.327
0.675	35.590	66.185	33.657	66.114	47.500	48.923
0.700	36.447	67.352	34.049	66.881	48.628	49.783
0.725	36.833	68.580	34.008	67.839	50.259	51.265

3.3.2 Effect of Changes in Rotation Rate

In contrast to the constant rotation rate case in Section 3.3.1, where the impact was greater at higher velocity, the constant flow rate case shows differences that are more significant at lower velocities, especially at lower flow rates. Figure 3-7 shows this effect by the spread of the curves, where negative values mean that the lower rotation value has a larger response in those regions. Remember that percent-change does not indicate the magnitude of the change. Refer to the spectra plots for magnitude changes. Over the region of interest, between 0.2 and 0.4 m/s, there is a large percent change in the 78 GPM case. This swing indicates that at the 0.2 m/s velocity the mixing performance is more sensitive to rotational rate than at the 0.4 m/s velocity. The lowest flow rate (58 GPM) goes through a similar transition at lower velocity (in the range of 0.1 to 0.2 m/s), while the highest flow rate (98 GPM) never shows this transition.

The influence of rotation rate is limited at the lower energy levels in the 43.2-inch and 120-inch models because the solid is not scaled. It will respond to absolute velocity levels when added to the CFD model. It is possible that, in real operations at the full-scale, a lower jet velocity with a different rotational rate could be more efficient, assuming that the maximum performance of the jet-mixer pumps is more than is needed. The data for Figure 3-7 is listed in Table 3-6.

Figure 3-7. Comparison of 120-Inch Cases at Constant GPM.

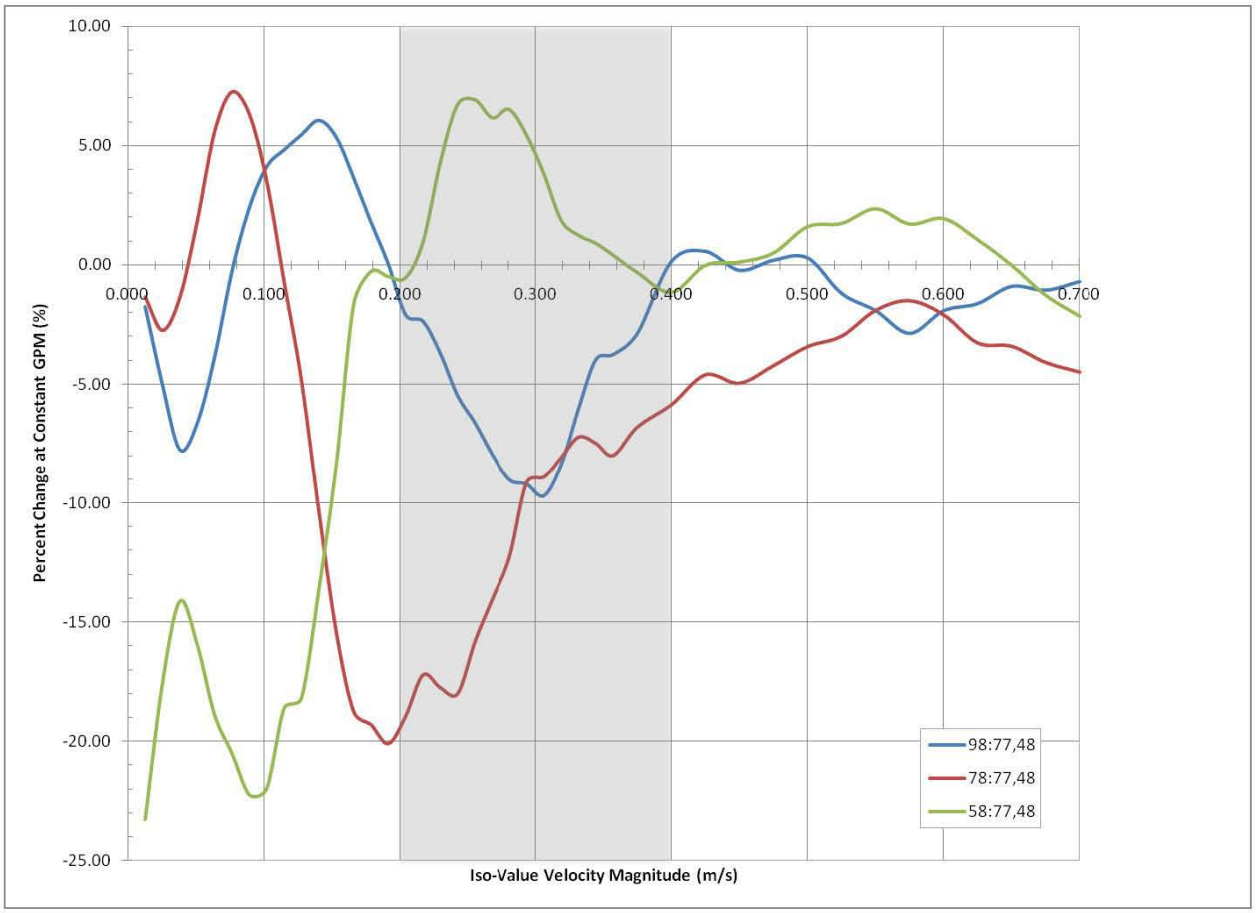

Table 3-6. Percent Change between Comparison Cases, Constant GPM (%) (2 pages).

Calculated from Iso-Value Surface Areas as 100(First-RPM - Second-RPM)/First-RPM*

Velocity Magnitude (m/s)	120-Inch RPM=0.77, RPM=0.48 at GPM=98 (%)	120-Inch RPM=0.77, RPM=0.48 at GPM=78 (%)	120-Inch RPM=0.77, RPM=0.48 at GPM=58 (%)
0.013	-1.741	-1.332	-23.275
0.026	-5.033	-2.737	-17.532
0.038	-7.746	-1.348	-14.119
0.051	-6.624	1.854	-15.951
0.064	-3.846	5.601	-18.894
0.077	-0.256	7.268	-20.508
0.089	2.409	6.328	-22.242
0.102	4.123	3.518	-21.968
0.115	4.827	-0.708	-18.602
0.128	5.458	-4.856	-18.174
0.140	6.057	-10.361	-13.632

Table 3-6. Percent Change between Comparison Cases, Constant GPM (%) (2 pages).

Calculated from Iso-Value Surface Areas as 100(First-RPM - Second-RPM)/First-RPM*

Velocity Magnitude (m/s)	120-Inch RPM=0.77, RPM=0.48 at GPM=98 (%)	120-Inch RPM=0.77, RPM=0.48 at GPM=78 (%)	120-Inch RPM=0.77, RPM=0.48 at GPM=58 (%)
0.153	5.352	-15.420	-8.389
0.166	3.653	-18.761	-1.654
0.179	1.794	-19.315	-0.261
0.191	0.041	-20.108	-0.476
0.204	-2.090	-18.952	-0.522
0.217	-2.353	-17.227	0.981
0.230	-3.708	-17.767	4.332
0.242	-5.480	-18.006	6.752
0.255	-6.614	-15.822	6.931
0.268	-7.945	-14.051	6.176
0.281	-9.009	-12.273	6.524
0.294	-9.196	-9.134	5.448
0.306	-9.680	-8.916	3.824
0.319	-8.373	-8.082	1.875
0.332	-6.006	-7.222	1.254
0.345	-3.949	-7.492	0.911
0.357	-3.743	-7.992	0.412
0.375	-2.860	-6.798	-0.309
0.400	0.151	-5.860	-1.143
0.425	0.573	-4.604	-0.006
0.450	-0.220	-4.957	0.125
0.475	0.201	-4.220	0.509
0.500	0.299	-3.419	1.614
0.525	-1.185	-2.983	1.748
0.550	-1.906	-1.898	2.367
0.575	-2.858	-1.494	1.722
0.600	-1.910	-2.088	1.953
0.625	-1.612	-3.267	1.064
0.650	-0.891	-3.406	-0.005
0.675	-1.052	-4.085	-1.264
0.700	-0.689	-4.488	-2.139
0.725	-0.497	-4.992	-2.869

4.0 SCALING RELATIONSHIPS AMONG THE THREE SCALES

In this section, the scaling among simulations at the full-scale, 120-inch scale and 43.2-inch scale is examined for similarity. Because each case is an exact scale (one third power law was used by the project), the behavior of one scale matches the other two scales. This relationship can be used to extrapolate the results of the denser sensitivity matrix completed for the 120-inch model to the full-scale and 43.2-inch scale.

4.1 Theory

The simulation run table (Table 3-1) supplied for work in FY-2011 assumes a one-third power scaling. Once the geometry scaling is specified as α in EQ 2 and EQ 3 below, the velocity scaling at the output face of the jet-mixer pump can be determined using EQ 4. The assumed GPM and RPM values can also be calculated using a one-third power scale because they conform to EQ 5, EQ 6, and EQ 7.

$$\alpha_s \equiv \frac{L_s}{L_{fs}} \qquad EQ\ 2$$

$$Volume \Rightarrow \alpha_s^3 \qquad EQ\ 3$$

$$Velocity \equiv \alpha_s^{1/3} = \frac{U_s}{U_{fs}} \qquad EQ\ 4$$

$$Time \Rightarrow \alpha_s^{2/3} = \frac{\frac{L_s}{L_{fs}}}{\frac{U_s}{U_{fs}}} = \alpha_s \alpha_s^{-1/3} \qquad EQ\ 5$$

$$InverseTime \Rightarrow \alpha_s^{-2/3} = \frac{rpm_s}{rpm_{fs}} \qquad EQ\ 6$$

$$\frac{GPM_s}{GPM_{fs}} = \alpha_s^3 \alpha_s^{-2/3} = \alpha_s^{7/3} \qquad EQ\ 7$$

$$\frac{W_s/V_s}{W_{fs}/V_{fs}} \equiv 1 \qquad EQ\ 8$$

$$W \equiv \frac{Kg}{s^3} m^2 \Rightarrow \qquad EQ\ 9$$

$$\left(\frac{Kg}{s}\right)_{ratio} \left(\frac{m}{s}\right)^2_{ratio} = \alpha_s^3 \Rightarrow \qquad EQ\ 10$$

$$\frac{U_s A_s \gamma_s}{U_{fs} A_{fs} \gamma_{fs}} \left(\frac{U_s}{U_{fs}}\right)^2 = \alpha_s^3 = \qquad EQ\ 11$$

$$\alpha_s^2 \left(\frac{U_s}{U_{fs}}\right)^3 = \alpha_s^3 \Rightarrow \qquad EQ\ 12$$

$$\therefore \left(\frac{U_s}{U_{fs}}\right) = \alpha_s^{1/3} \qquad EQ\ 13$$

Other possible ways to scale other than constant power per unit volume include the time to turn over the tank volume, the time that the jet flow takes to go from the pump to the tank wall, or the circulation time for a pump return circuit. These times are also important in terms of mixing performance. There is no solid phase in the model (it is liquid only), but the time it takes a solid particle to fall the height of the tank would also be unconstrained by the scaling specified. The scaling equations are useful when correcting for small variations in actual flow rate versus intended flow rate in simulations and model test runs. For example, the 120-inch model run needed to be remapped when scaled to compare with the other two scales because the jet-face velocity was unintentionally too high. Adjustment factors are scaled per EQ 4 to obtain corrected iso-value velocity magnitude and iso-value surface area correlations between full-scale and the smaller 120-inch and 43.2-inch models.

Part of the work in FY-2011 has included testing the hypothesis that if more extensive sensitivity matrices of simulations are carried out at a single scale (120-inch), those results apply at all scales because single-phase flow will follow the scaling laws to sufficient accuracy. More information about the flow response to jet-mixer pumps is obtained by looking at variations in pumping rate, rotation speed and orifice size (velocity at the jet face), than by repeating simulations at precisely the same flow configurations, given precise scaling relationships, in separate models.

For example, if the assumed scaling is not quite right for the actual process (e.g. with solid included), a denser matrix allows interpolation of the results using a different set of scaling equations without re-running all the simulations with differing assumptions.

4.1.1 Power per Unit Volume

Besides the straight geometric scaling (α), equal power per volume between the scales was assumed by the project. To see this assumption, a derivation of the one-third scaling of velocity (U) is shown in EQ 8 through EQ 13. The hypothesis is given by EQ 8 where W is power and V is volume. The subscripts refer to "scale" and "full-scale." EQ 9 gives the definition of power in more fundamental units. Equation 9 is put in EQ 8 and the distributive and associative properties are used to rearrange it into EQ 10, where the subscript "ratio" means that the same form has an "s" group over an "fs" group. Equation 11 assumes incompressible flow to get the mass flow where "A" is the area for the nozzle face and γ is density (same for all scales). Equation 12 and EQ 13 gather all common terms and show reduction to final form and the deviation is complete. The one-third scaling of velocity is a consequence of the equal power per volume assumption.

4.2 Full, 120-Inch, and 43.2-Inch Scale Comparison

Figure 4-1 of the scaled (i.e. using full-scale units) iso-value area versus absolute velocity magnitude (unscaled) shows a single peak of approximately the same magnitude for all three scales. The peak is located further left and becomes sharper (smaller velocity magnitudes) as the size of the model decreases.

Note that Table 4-1, which lists the data using Figure 4-1, has gaps because the mapping used for the smaller scales differ, such that the smaller models hit their scaled version of 0.7 m/s at lower absolute values. At that point, the values chosen begin to match those chosen for the full scale (and the gaps in the table disappear). The values at each scale were chosen to make the next step, scaling velocity magnitude, straight forward.

Figure 4-1. Comparison Cases for each of the Scales (actual simulations).

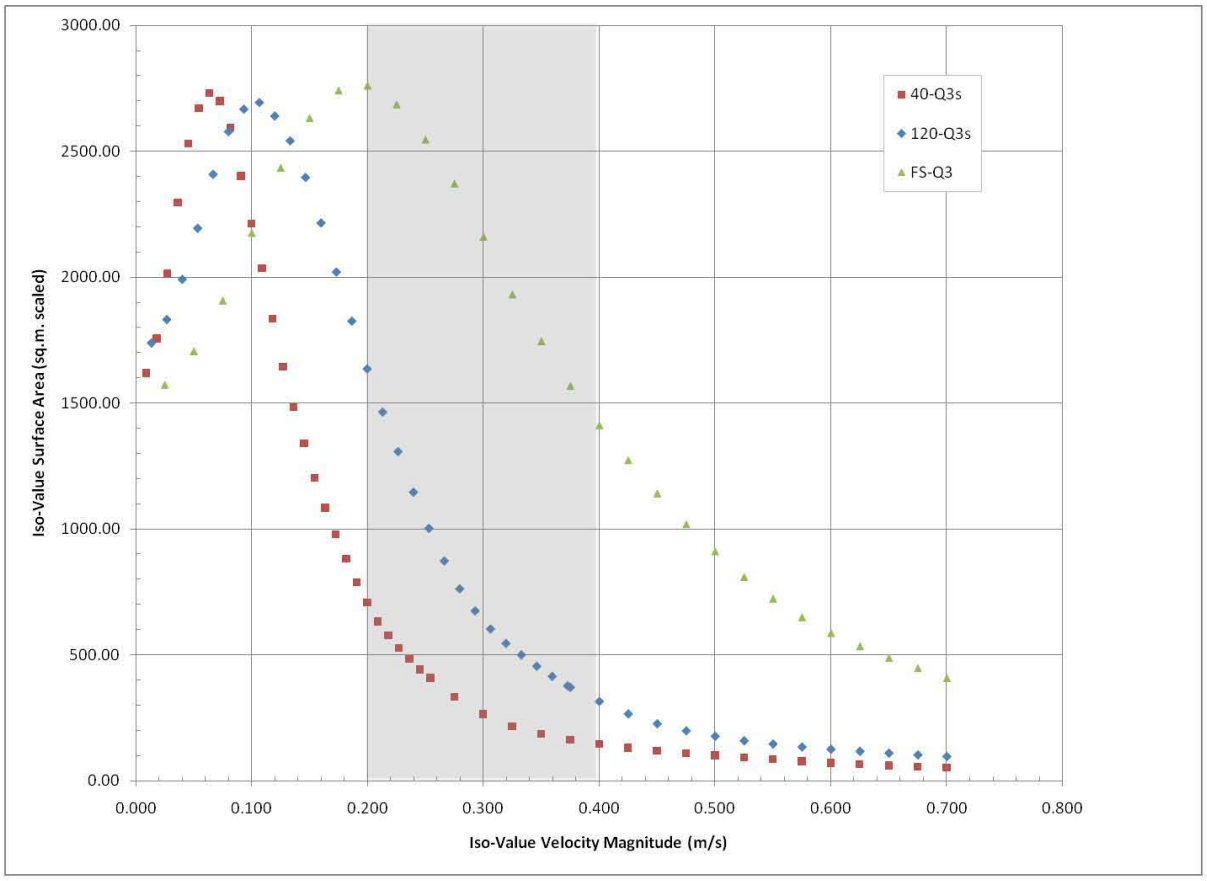

Table 4-1. Iso-Value Surface Area (scaled) versus Velocity Magnitude (3 pages).

Comparison Runs

Velocity Magnitude (m/s)	Full-Scale GPM=10400 RPM=0.2 Q3 (sq. m.)	120-Inch GPM=98 RPM=0.77 Q3 (sq. m.)	43.2-Inch GPM=8.6 RPM=1.51 Q3 (sq. m.)
0.009			1618.52
0.013		1738.17	
0.018			1756.69
0.025	1572.67		
0.027		1830.80	
0.027			2013.70
0.036			2296.86
0.040		1990.33	
0.045			2529.98
0.050	1705.74		
0.053		2193.37	
0.055			2671.02
0.064			2730.40
0.067		2407.49	
0.073			2699.22
0.075	1907.68		
0.080		2576.89	
0.082			2593.79
0.091			2401.95
0.093		2666.18	
0.100			2213.50
0.100	2176.25		
0.106		2692.52	
0.109			2034.55
0.118			1833.80
0.120		2639.10	
0.125	2435.04		
0.127			1643.45
0.133		2540.59	
0.136			1483.81
0.140			
0.145			1340.34
0.146		2395.46	
0.150	2632.66		
0.154			1203.48

Table 4-1. Iso-Value Surface Area (scaled) versus Velocity Magnitude (3 pages).

Comparison Runs

Velocity Magnitude (m/s)	Full-Scale GPM=10400 RPM=0.2 Q3 (sq. m.)	120-Inch GPM=98 RPM=0.77 Q3 (sq. m.)	43.2-Inch GPM=8.6 RPM=1.51 Q3 (sq. m.)
0.160		2214.42	
0.164			1084.12
0.173			979.02
0.173		2019.66	
0.175	2742.35		
0.182			881.03
0.186		1824.75	
0.191			788.79
0.200		1635.10	
0.200			706.78
0.200	2761.78		
0.209			632.82
0.213		1463.80	
0.218			576.46
0.225	2687.10		
0.226		1306.91	
0.227			527.34
0.236			483.16
0.240		1145.59	
0.245			441.80
0.250	2547.40		
0.253		1002.21	
0.254			408.70
0.266		872.48	
0.275	2372.50		331.95
0.279		762.02	
0.293		674.35	
0.300	2161.09		263.97
0.306		602.60	
0.319		545.41	
0.325	1931.98		214.92
0.333		499.48	
0.346		454.63	
0.350	1746.03		186.63
0.359		414.62	

Table 4-1. Iso-Value Surface Area (scaled) versus Velocity Magnitude (3 pages).

Comparison Runs

Velocity Magnitude (m/s)	Full-Scale GPM=10400 RPM=0.2 Q3 (sq. m.)	120-Inch GPM=98 RPM=0.77 Q3 (sq. m.)	43.2-Inch GPM=8.6 RPM=1.51 Q3 (sq. m.)
0.373		376.80	
0.375	1568.11	370.82	163.51
0.400	1411.88	314.64	145.27
0.425	1272.77	265.70	130.69
0.450	1141.11	226.08	119.34
0.475	1018.58	198.35	109.55
0.500	910.44	176.60	100.80
0.525	808.61	158.91	92.34
0.550	722.53	145.71	84.60
0.575	649.08	134.01	77.56
0.600	586.31	125.32	70.41
0.625	533.63	116.79	64.68
0.650	486.96	109.72	59.90
0.675	446.74	102.53	55.86
0.700	406.62	96.30	51.85

If the iso-value velocity magnitude is also scaled, the curves converge to a reasonable approximation of one another, considering the statistical nature of the process, as shown in Figure 4-2. The process could be made better if the simulations were re-run with exactly the same mesh and corrected velocities at the pump nozzle, etc. For Figure 4-2, both the 43.2-inch tank results and the 120-inch tank results are scaled up to the full-scale area units to show a comparison. The same set of curves would have been obtained if the full-scale and 120-inch tank results were scaled down to the 43.2-inch tank scale before comparison. The conclusion is that smaller-scale models can "look" the same as full-scale models if scaled properly for single-fluid simulations. This conclusion is used to generate tables at multiple scales from the 120-inch model sensitivity simulations discussed in Section 3.0 (mainly because the 120-inch simulations were farther ahead and that particular model was running faster). This extrapolation applies only to the flow of liquid in the tank, because any solid phase will in all likelihood scale differently and respond to absolute velocity, not scaled velocity. In any case, in the current application, the solid phase is not present and all particle motions are assumed based upon defined fluid velocities. However, confidence that has been gained in the present CFD work allows the isolation of the differing scaling presented by inclusion of the solid. Unfortunately, at present, the constitutive relationships between the multiple phases of the full-scale mixture are largely unknown. Further work with CFD may be able to tease out a model for the solid-fluid interaction by analyzing detailed results for the on-going physical-model tests. The data used in Figure 4-2 are listed in Table 4-2.

Figure 4-2. Comparison Cases for All Models

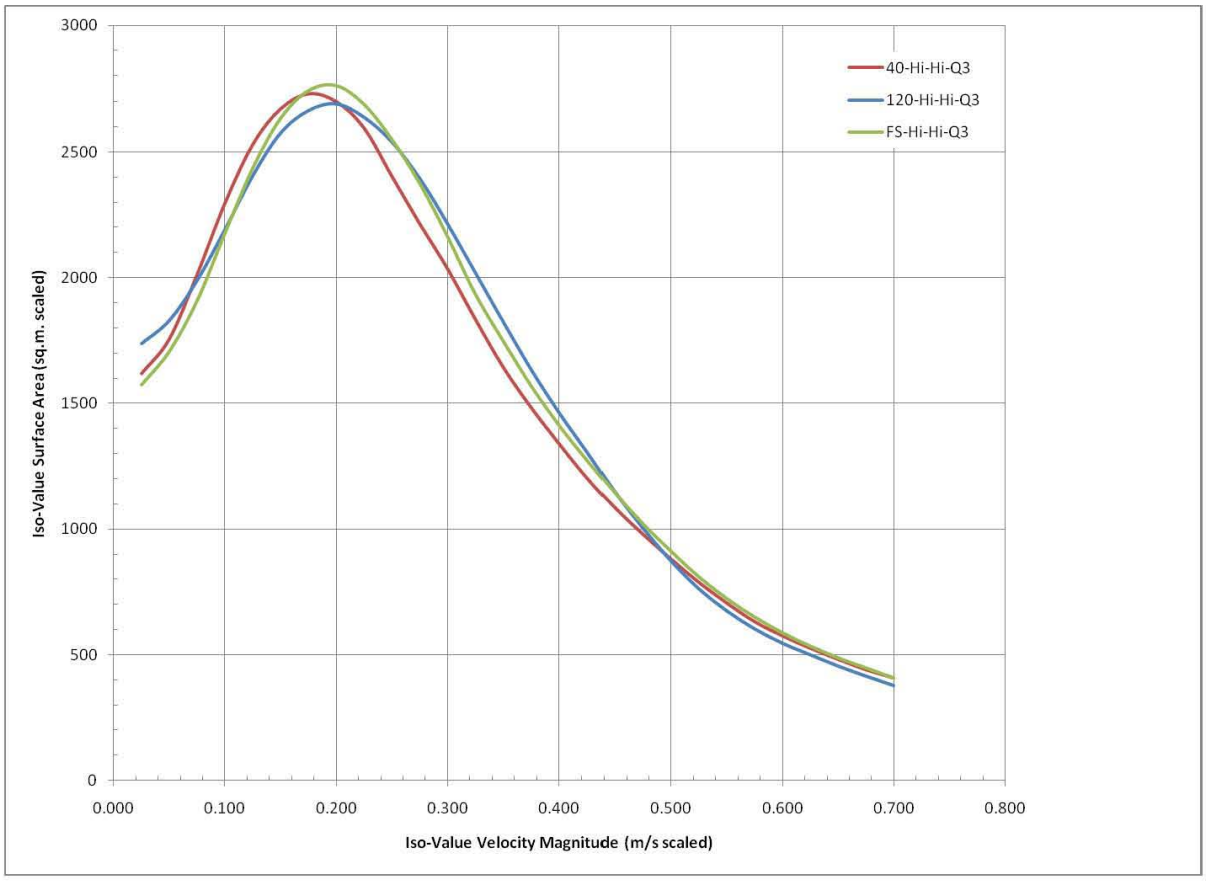

Table 4-2. Iso-Value Surface Area (scaled) versus Velocity Magnitude (scaled) (2pages).

Comparison Runs

Velocity Magnitude (m/s)	Full-Scale GPM=10400 / RPM=0.2 Q3 (sq. m.)	120-Inch GPM=98 / RPM=0.77 Q3 (sq. m.)	43.2-Inch GPM=8.6 / RPM=1.51 Q3 (sq. m.)
0.025	1572.67	1738.17	1618.52
0.050	1705.74	1830.80	1756.69
0.075	1907.68	1990.33	2013.70
0.100	2176.25	2193.37	2296.86
0.125	2435.04	2407.49	2529.98
0.150	2632.66	2576.89	2671.02
0.175	2742.35	2666.18	2730.40
0.200	2761.78	2692.52	2699.22
0.225	2687.10	2639.10	2593.79
0.250	2547.40	2540.59	2401.95

Table 4-2. Iso-Value Surface Area (scaled) versus Velocity Magnitude (scaled) (2pages).

Comparison Runs

Velocity Magnitude (m/s)	Full-Scale GPM=10400 / RPM=0.2 Q3 (sq. m.)	120-Inch GPM=98 / RPM=0.77 Q3 (sq. m.)	43.2-Inch GPM=8.6 / RPM=1.51 Q3 (sq. m.)
0.275	2372.50	2395.46	2213.50
0.300	2161.09	2214.42	2034.55
0.325	1931.98	2019.66	1833.80
0.350	1746.03	1824.75	1643.45
0.375	1568.11	1635.10	1483.81
0.400	1411.88	1463.80	1340.34
0.425	1272.77	1306.91	1203.48
0.450	1141.11	1145.59	1084.12
0.475	1018.58	1002.21	979.02
0.500	910.44	872.48	881.03
0.525	808.61	762.02	788.79
0.550	722.53	674.35	706.78
0.575	649.08	602.60	632.82
0.600	586.31	545.41	576.46
0.625	533.63	499.48	527.34
0.650	486.96	454.63	483.16
0.675	446.74	414.62	441.80
0.700	406.62	376.80	408.70

Figure 4-3 shows the difference among the three scales, after all scaling is done, as a percent change (percent-change does not indicate magnitude of difference, etc.), which emphasizes the small differences seen in Figure 4-2. Small errors still exist due to the inherent variability of the process as well as small differences in intended and resulting injection velocity at the jet faces (the outflow is a pressure condition, uncoupled with the jet face) in the CFD model. The differences are about 10% or less, even considering the statistical variation. Therefore, scaling from the 120-inch scale sensitivity cases will be adequate until individual simulations for full-scale and 43.2-inch scale can be completed or the solid phase added to the CFD model. The data used in Figure 4-3 are listed in Table 4-3.

Figure 4-3. Distribution of Differences Three Cross-Cases.

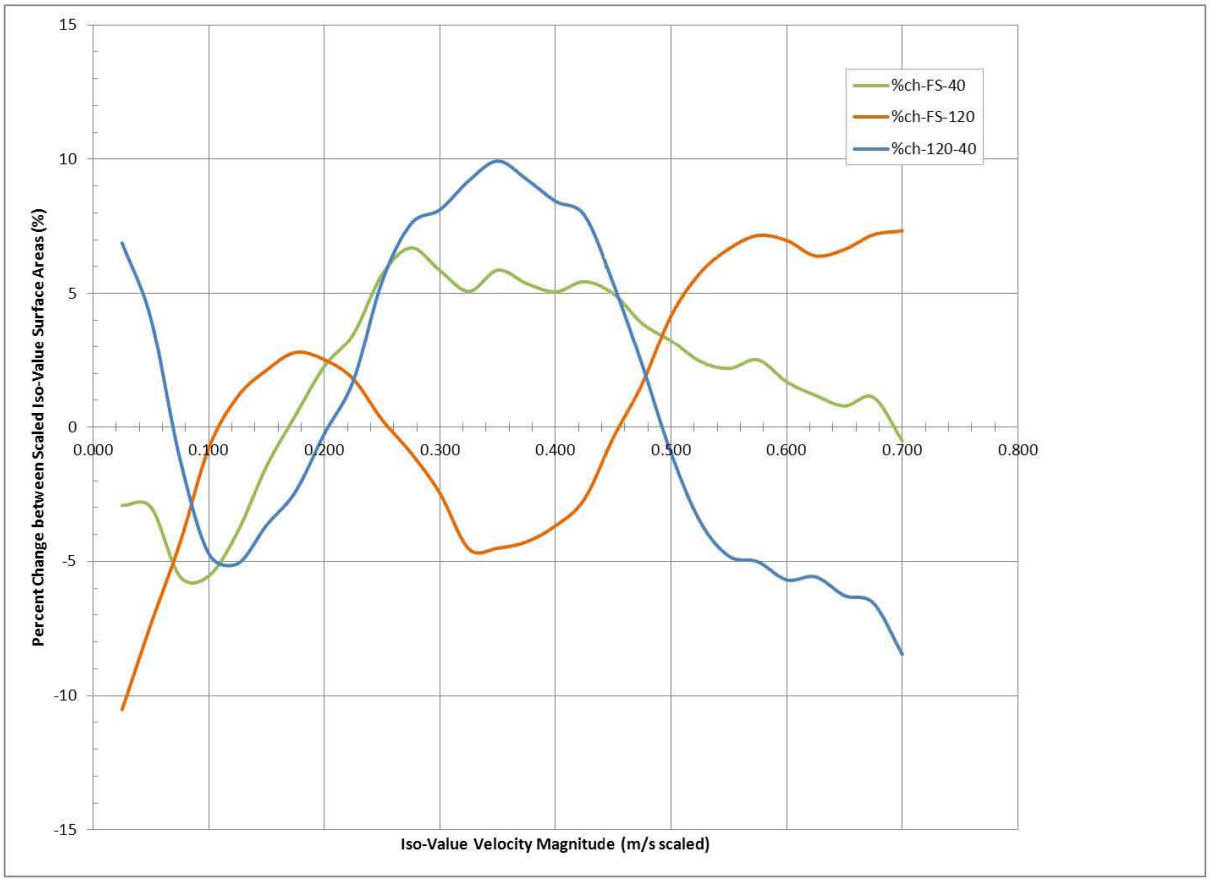

Table 4-3. Percent Change between Comparison Cases (%) (2 pages).

Calculated from 100(First-Value - Second-Value)/First-Value*

Velocity Magnitude (m/s)	Full-Scale vs 43.2-Inch	Full-Scale vs 120-Inch	120-Inch vs 43.2-Inch
0.025	-2.916	-10.523	6.884
0.050	-2.987	-7.332	4.048
0.075	-5.557	-4.332	-1.174
0.100	-5.542	-0.787	-4.718
0.125	-3.899	1.131	-5.088
0.150	-1.457	2.118	-3.653
0.175	0.436	2.777	-2.409
0.200	2.266	2.508	-0.249
0.225	3.473	1.786	1.717
0.250	5.710	0.267	5.457
0.275	6.702	-0.968	7.596
0.300	5.855	-2.468	8.123

Table 4-3. Percent Change between Comparison Cases (%) (2 pages).

Calculated from 100(First-Value - Second-Value)/First-Value*

Velocity Magnitude (m/s)	Full-Scale vs 43.2-Inch	Full-Scale vs 120-Inch	120-Inch vs 43.2-Inch
0.325	5.082	-4.539	9.203
0.350	5.875	-4.508	9.936
0.375	5.376	-4.272	9.253
0.400	5.067	-3.677	8.434
0.425	5.443	-2.682	7.914
0.450	4.994	-0.393	5.366
0.475	3.884	1.608	2.314
0.500	3.231	4.169	-0.980
0.525	2.451	5.761	-3.513
0.550	2.179	6.669	-4.810
0.575	2.505	7.160	-5.014
0.600	1.679	6.975	-5.694
0.625	1.179	6.399	-5.577
0.650	0.782	6.641	-6.275
0.675	1.106	7.190	-6.555
0.700	-0.512	7.334	-8.466

4.3 Scaling 120-Inch Cases to Full-Scale and 43.2-Inch Scales

In this section, the 120-inch results are extrapolated to full-scale and 43.2-inch scale by scaling the iso-value surface area, while the iso-value velocity magnitude remains unchanged (but transformed via scaling). The comparison cases discussed in Section 4.2 do not match exactly, because Table 4-5 and associated figures use straight geometric scaling (used consistently for the 120-inch models), as shown in Equations 2 through 7. Small errors in intended versus actual flow rates in the 120-inch scale are not accounted for (as was done in Section 4.2). This condition makes Table 4-5 and the figures consistent, as all the cases use the same iso-value velocity magnitude mapping, but at odds with Section 4.2, which is addressed in Table 4-4 and Figure 4-4.

Because absolute velocity magnitude is used as a scale, the table has holes again so the curves are shown with symbols since Microsoft Excel seems inadequate to fitting curves through the lines when the values aren't all at the same points on the horizontal axis.

In Figure 4-4, the same mapping used in Section 4.2 is used to compare extrapolation of the 120-inch model in that section with the simulation results for the full-scale and 43.2-inch scales. The data for Figure 4-4 is in Table 4-4.

Figure 4-4. Results at Maximum GPM and Maximum RPM Case (Consistent with Sect. 4.2).

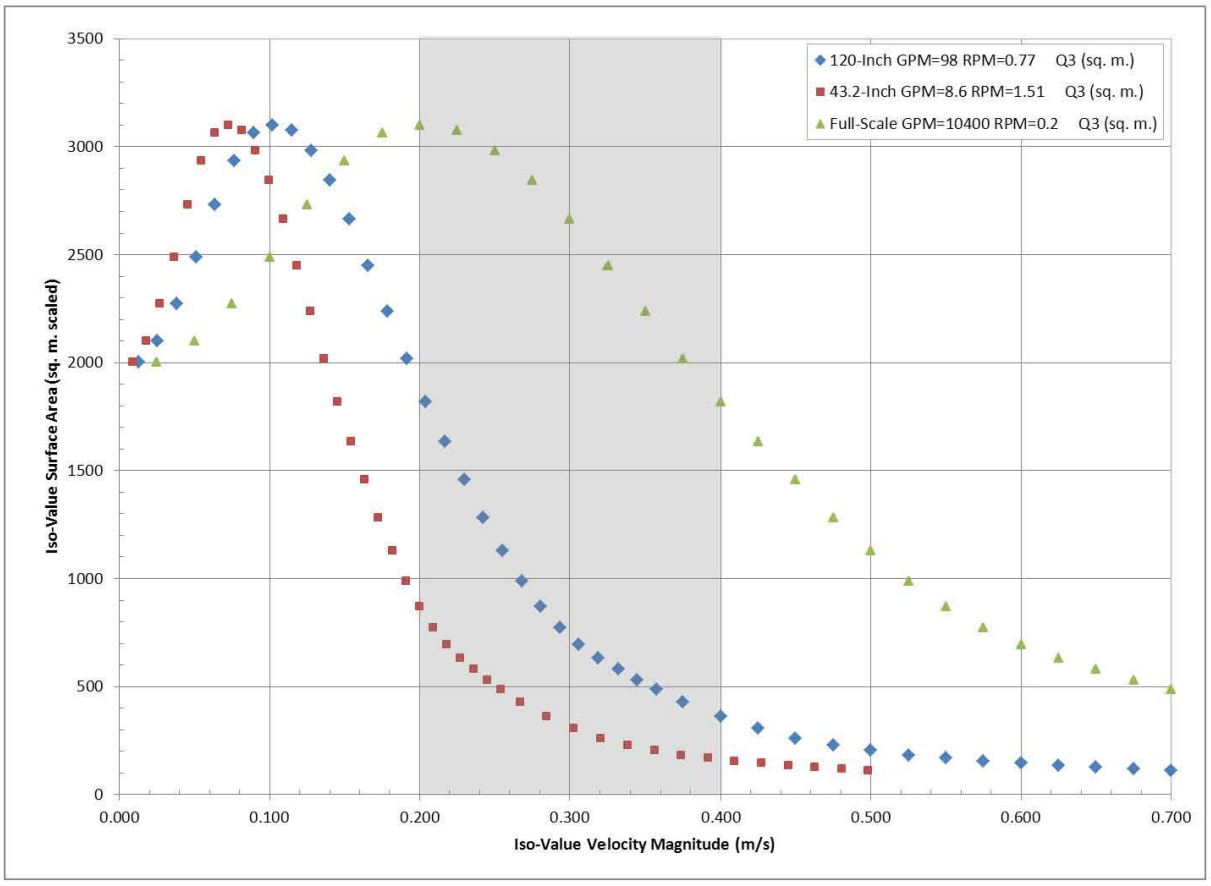

Table 4-4. Iso-Value Surface Area (scaled) versus Velocity Magnitude (4 pages).

Compare extrapolated 120-inch scale results to full-scale and 43.2-inch scale results.					
All Results scaled to Full Scale Units for Comparison					
Velocity Magnitude (m/s)	**120-Inch GPM=98 RPM=0.77 Q3 (sq. m.)**	**Full-Scale Extrapolated from 120-inch Case (sq. m.)**	**Full-Scale GPM=10400 RPM=0.2 Q3 (sq. m.)**	**43.2-Inch Extrapolated from 120-inch Case (sq. m.)**	**43.2-Inch GPM=8.6 RPM=1.51 Q3 (sq. m.)**
0.009				1738.17	1618.52
0.013	1738.17				
0.018				1830.80	1756.69
0.025		1738.17	1572.67		
0.027					
0.027	1830.80			1990.33	2013.70

Table 4-4. Iso-Value Surface Area (scaled) versus Velocity Magnitude (4 pages).

Compare extrapolated 120-inch scale results to full-scale and 43.2-inch scale results.					
All Results scaled to Full Scale Units for Comparison					
Velocity Magnitude (m/s)	120-Inch GPM=98 RPM=0.77 Q3 (sq. m.)	Full-Scale Extrapolated from 120-inch Case (sq. m.)	Full-Scale GPM=10400 RPM=0.2 Q3 (sq. m.)	43.2-Inch Extrapolated from 120-inch Case (sq. m.)	43.2-Inch GPM=8.6 RPM=1.51 Q3 (sq. m.)
0.036				2193.37	2296.86
0.040	1990.33				
0.045				2407.49	2529.98
0.050		1830.80	1705.74		
0.053	2193.37				
0.055				2576.89	2671.02
0.064				2666.18	2730.40
0.067	2407.49				
0.073				2692.52	2699.22
0.075		1990.33	1907.68		
0.080	2576.89				
0.082				2639.10	2593.79
0.091				2540.59	2401.95
0.093	2666.18				
0.100		2193.37	2176.25	2395.46	2213.50
0.106	2692.52				
0.109				2214.42	2034.55
0.118				2019.66	1833.80
0.120	2639.10				
0.125		2407.49	2435.04		
0.127				1824.75	1643.45
0.133	2540.59				
0.136				1635.10	1483.81
0.145				1463.80	1340.34
0.146	2395.46				
0.150		2576.89	2632.66		
0.154				1306.91	1203.48
0.160	2214.42				
0.164				1145.59	1084.12
0.173	2019.66			1002.21	979.02
0.175		2666.18	2742.35		
0.182				872.48	881.03

Table 4-4. Iso-Value Surface Area (scaled) versus Velocity Magnitude (4 pages).

Compare extrapolated 120-inch scale results to full-scale and 43.2-inch scale results.					
All Results scaled to Full Scale Units for Comparison					
Velocity Magnitude (m/s)	120-Inch GPM=98 RPM=0.77 Q3 (sq. m.)	Full-Scale Extrapolated from 120-inch Case (sq. m.)	Full-Scale GPM=10400 RPM=0.2 Q3 (sq. m.)	43.2-Inch Extrapolated from 120-inch Case (sq. m.)	43.2-Inch GPM=8.6 RPM=1.51 Q3 (sq. m.)
0.186	1824.75				
0.191				762.02	788.79
0.200	1635.10	2692.52	2761.78	674.35	706.78
0.209				602.60	632.82
0.213	1463.80				
0.218				545.41	576.46
0.225		2639.10	2687.10		
0.226	1306.91				
0.227				499.48	527.34
0.236				454.63	483.16
0.240	1145.59				
0.245				414.62	441.80
0.250		2540.59	2547.40		
0.253	1002.21				
0.254				376.80	408.70
0.256				370.82	
0.266	872.48				
0.273				314.64	
0.275		2395.46	2372.50		
0.279	762.02				331.95
0.290				265.70	
0.293	674.35				
0.300		2214.42	2161.09		
0.306	602.60				263.97
0.307				226.08	
0.319	545.41				
0.324				198.35	
0.325		2019.66	1931.98		
0.333	499.48				214.92
0.341				176.60	
0.346	454.63				
0.350		1824.75	1746.03		

Table 4-4. Iso-Value Surface Area (scaled) versus Velocity Magnitude (4 pages).

Compare extrapolated 120-inch scale results to full-scale and 43.2-inch scale results.					
All Results scaled to Full Scale Units for Comparison					
Velocity Magnitude (m/s)	120-Inch GPM=98 RPM=0.77 Q3 (sq. m.)	Full-Scale Extrapolated from 120-inch Case (sq. m.)	Full-Scale GPM=10400 RPM=0.2 Q3 (sq. m.)	43.2-Inch Extrapolated from 120-inch Case (sq. m.)	43.2-Inch GPM=8.6 RPM=1.51 Q3 (sq. m.)
0.358				158.91	186.63
0.359	414.62				
0.373	376.80				
0.375	370.82	1635.10	1568.11		
0.376				145.71	163.51
0.393				134.01	
0.400	314.64	1463.80	1411.88		
0.410				125.32	145.27
0.425	265.70	1306.91	1272.77		
0.427				116.79	130.69
0.444				109.72	
0.450	226.08	1145.59	1141.11		
0.461				102.53	119.34
0.475	198.35	1002.21	1018.58		
0.478				96.30	109.55
0.500	176.60	872.48	910.44		
0.525	158.91	762.02	808.61		100.80
0.550	145.71	674.35	722.53		92.34
0.575	134.01	602.60	649.08		84.60
0.600	125.32	545.41	586.31		77.56
0.625	116.79	499.48	533.63		70.41
0.650	109.72	454.63	486.96		64.68
0.675	102.53	414.62	446.74		59.90
0.700	96.30	376.80	406.62		55.86

Figure 4-5 shows the frequency analogy-shift with scale as the scaled 120-inch tank results are transformed to the full-scale and 43.2-inch scale cases at the highest flow rate and fastest pump rotational rate values used for comparison with actual CFD simulations. The values for each scale are listed in the legend. The legend items with –ext are the scaled results and the legend items with Q3 or Q3s are the actual model results. The close correlation between the scaled results and the modeled results demonstrate the functionality of scaling results based on the 120-inch scale model.

Figure 4-5. Extrapolated versus Simulated.

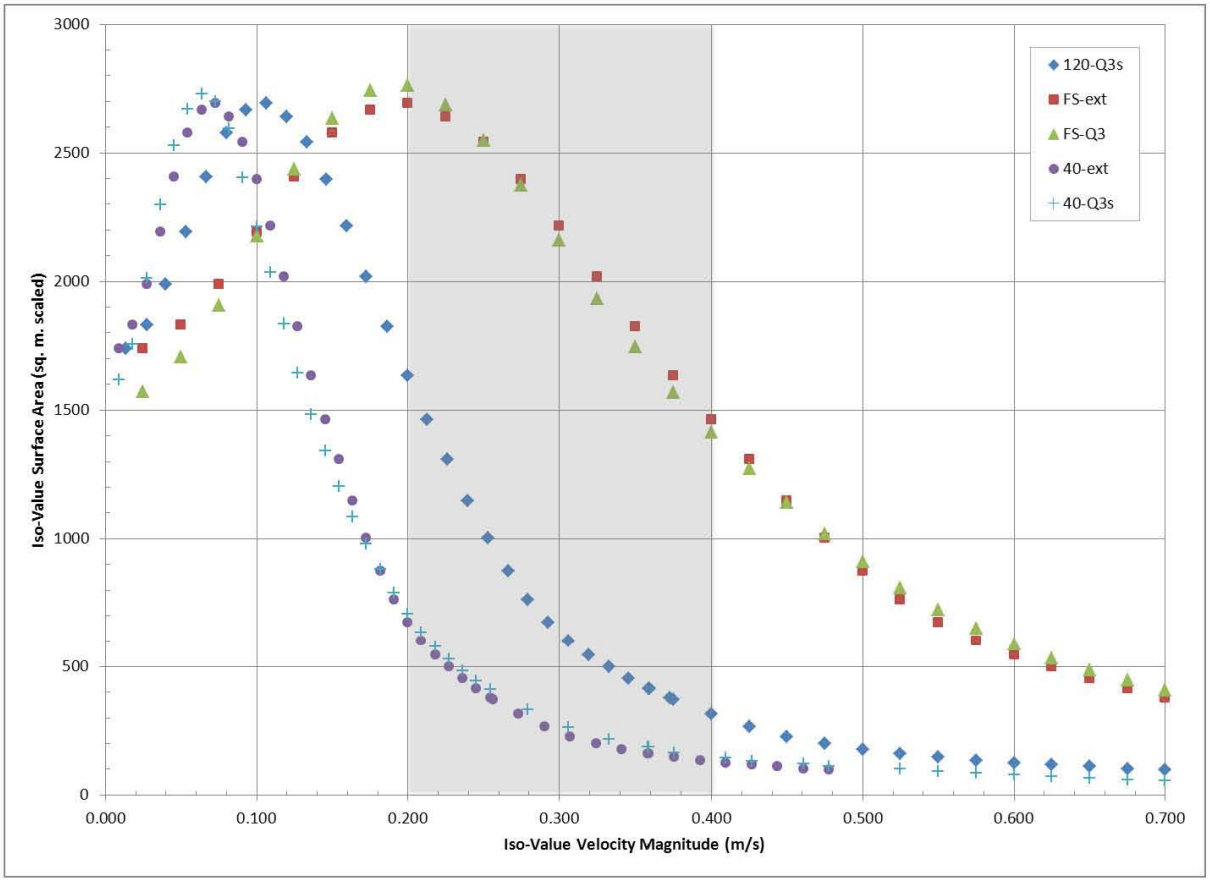

In Figure 4-6, the matching cases for maximum flow rate and minimum rotational rate are shown. The effect is a subtle shift in the peaks toward lower frequency (i.e. iso-value velocity magnitude). The peaks also become slightly sharper.

Figure 4-6. Maximum GPM and Minimum RPM Case.

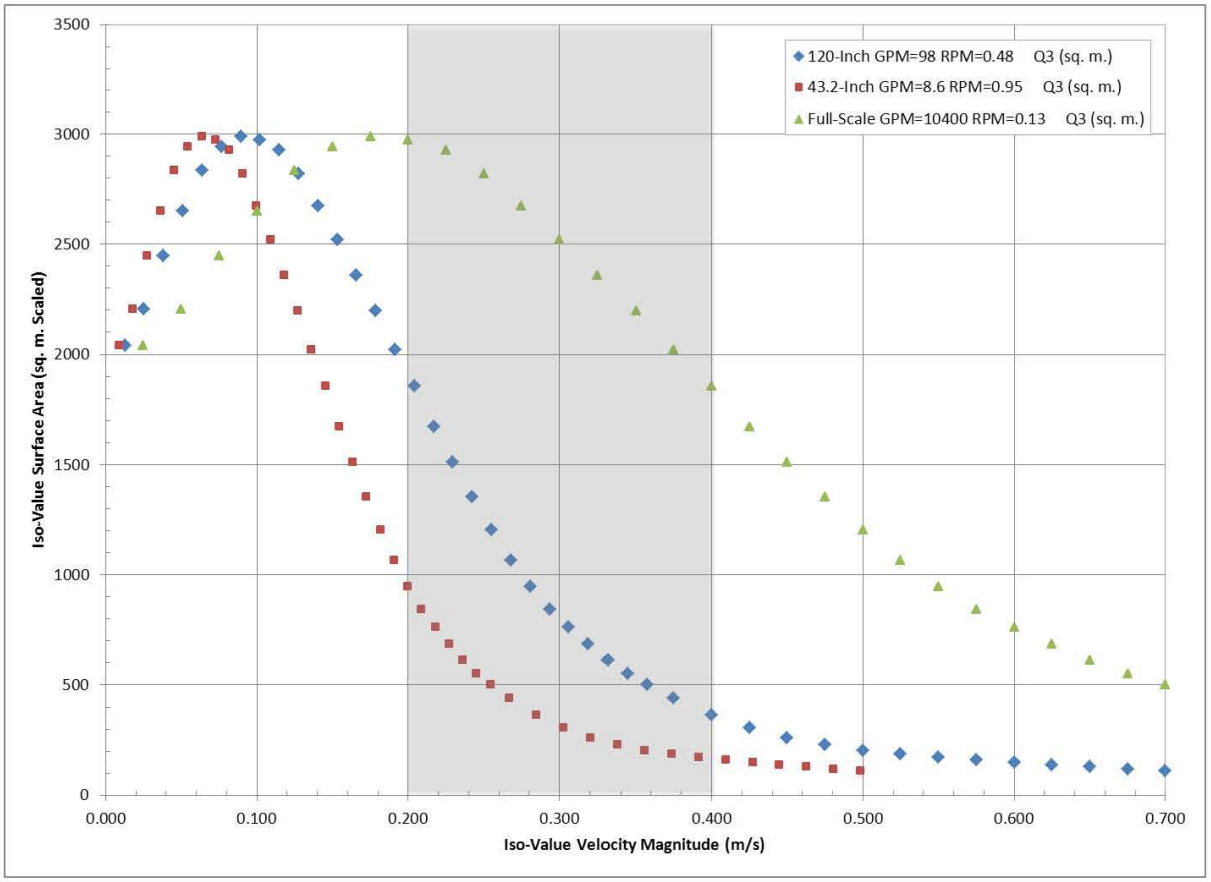

Figure 4-7 shows the medium flow rate, maximum pump rotational rate case, which also emphasizes the leftward shift of the peaks as flow rate decreases. This shift means that the volume of the tank excited to high velocity has decreased and more fluid is circulating at lower average velocities. The magnitude of the peak has fallen as well.

Figure 4-7. Medium GPM and Maximum RPM Case

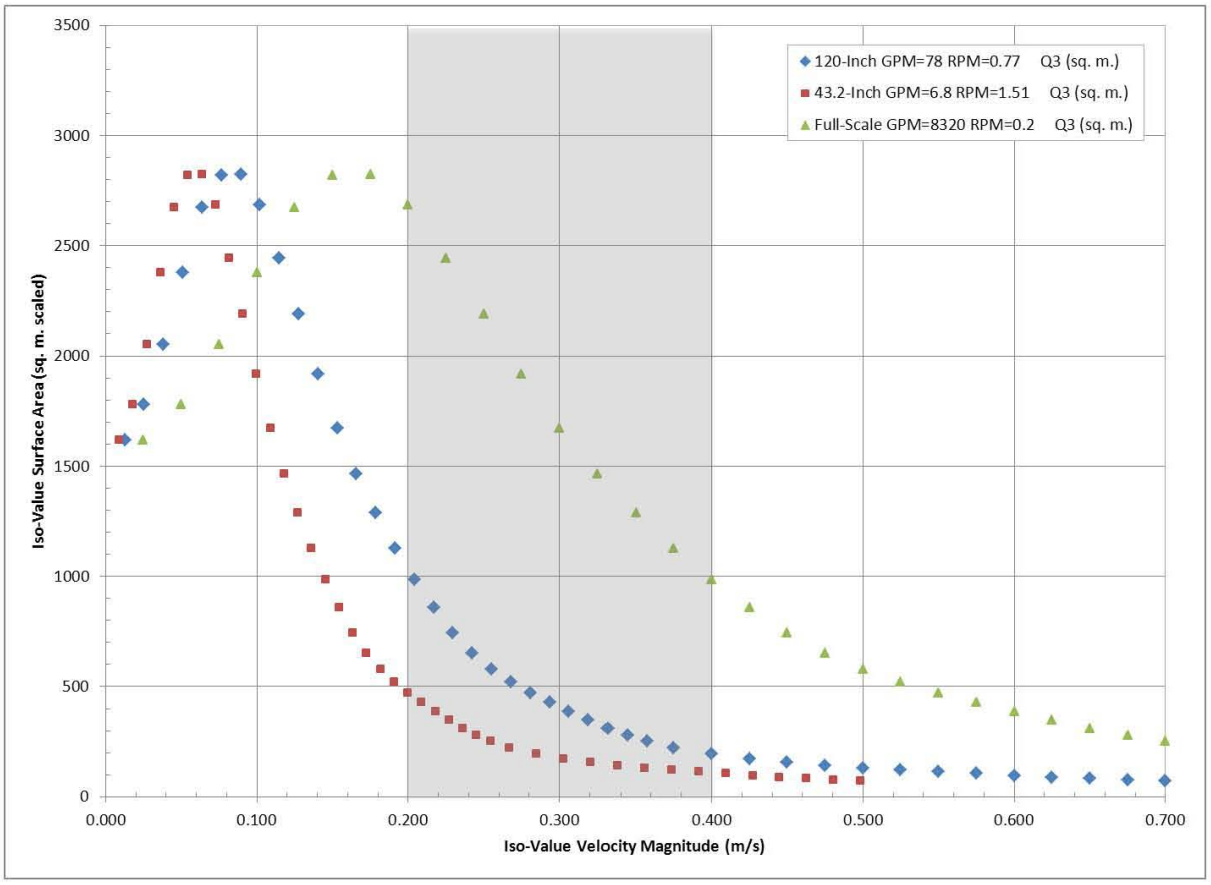

Figure 4-8 shows the effect of reduction in rotation speed when flow rate is at the medium setting. The interesting thing to note in the figure is that more energy is injected in the higher iso-value velocity magnitude level. This high energy can be seen by noting the level at which the full-scale curve crosses the 0.4 m/s line in Figure 4-7 versus Figure 4-8. The higher RPM crosses at a lower value of iso-value surface area. Therefore, under these conditions, a slower rotation speed helps spread fluid velocity into more volume of the tank.

Figure 4-8. Medium GPM and Minimum RPM Case.

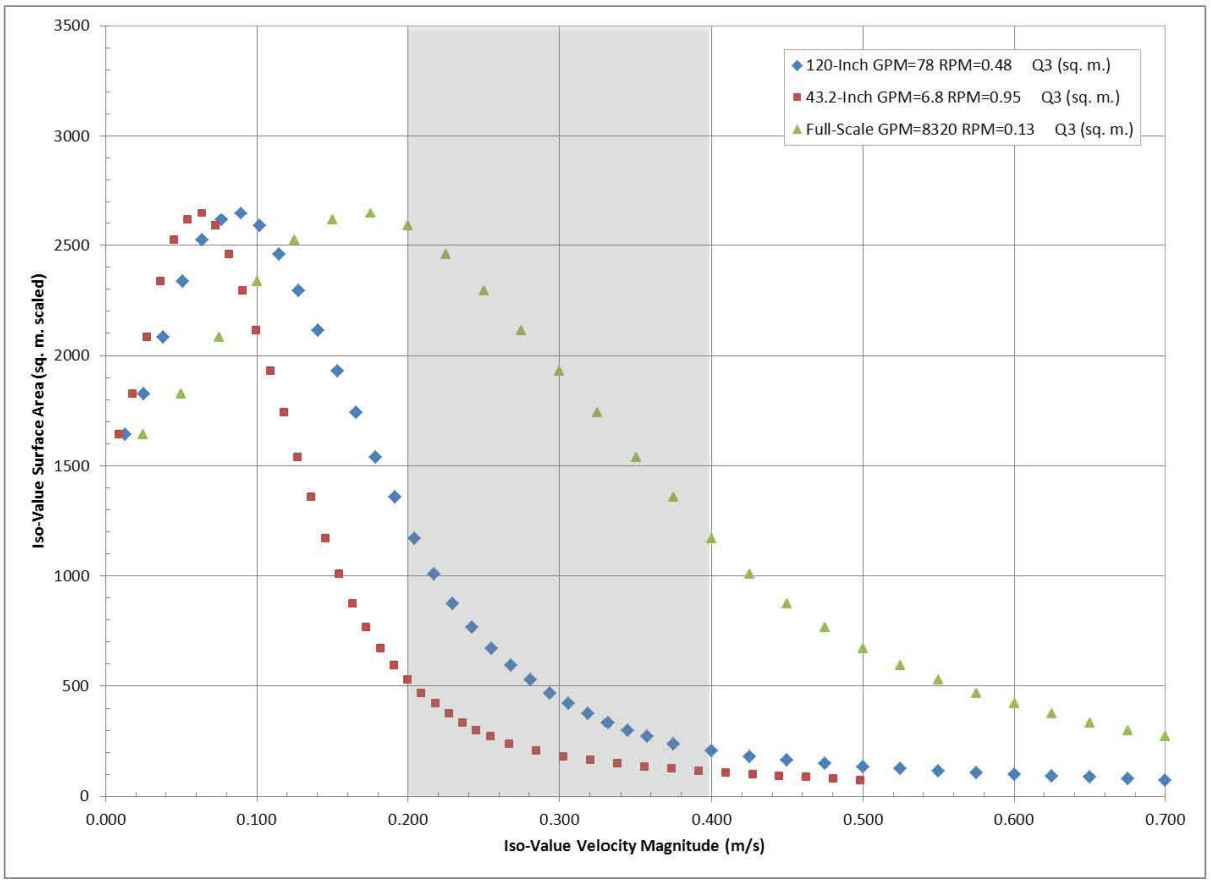

Figure 4-9 and Figure 4-10 show the results of lowering the flow rate to its minimum. Once again, the zero crossing of the full-scale curve at a value of 0.2 m/s shows that the lower rotation speed is more effective at pushing higher fluid velocities into the interior. The peaks continue to shift leftward. However, the peaks are quite high because most of the energy put in at the lower flow rate is settling at a relatively low iso-value velocity magnitude.

Figure 4-9. Minimum GPM and Maximum RPM Case.

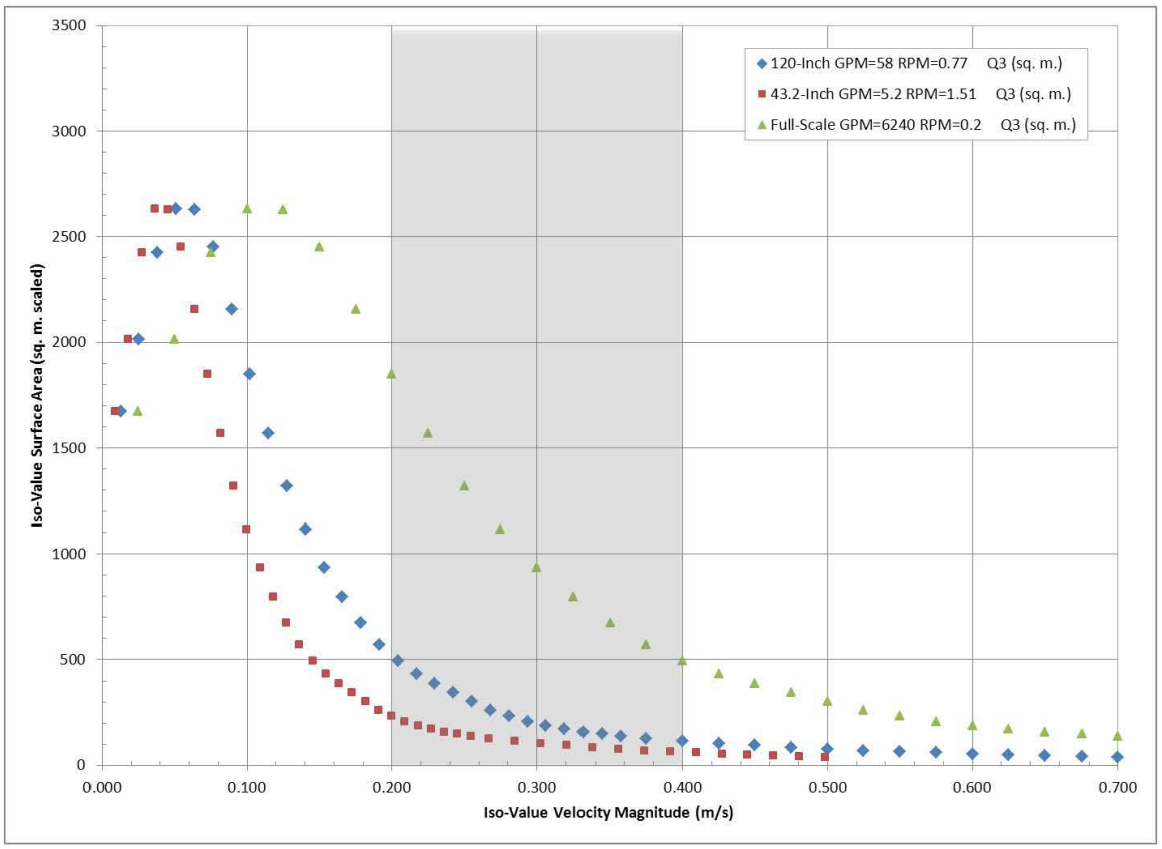

Figure 4-10. Minimum GPM and Minimum RPM Case.

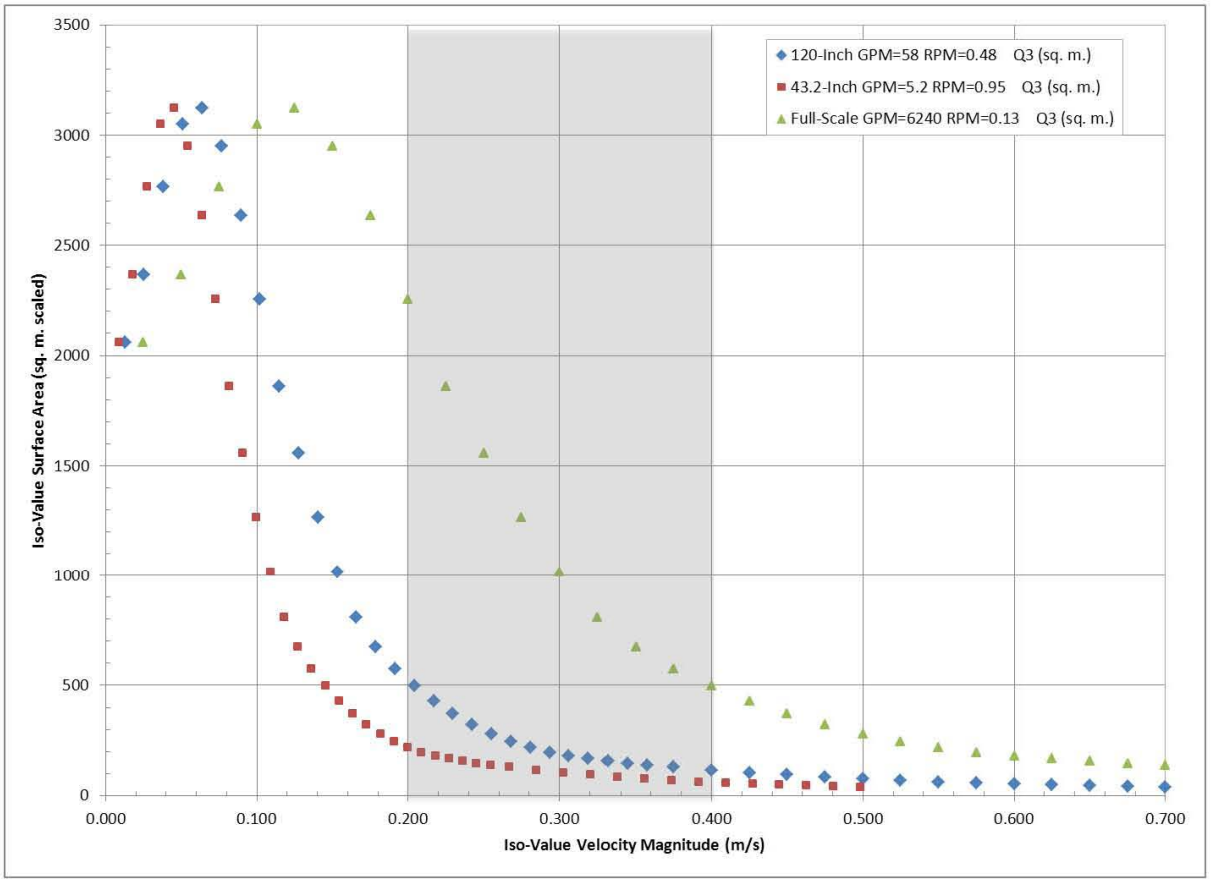

All of the results shown in Figure 4-6 through Figure 4-10 are listed in Table 4-5. There are gaps in the table due to the mapping of iso-value velocity magnitude between the scales. Specifically, the first 28 values of each column represent perfect scaling. This scaling takes the 120-inch model up to the equivalent of 0.7 iso-value velocity magnitude at full-scale. The tail of the 43.2-inch stops short of this value because values beyond 0.7 m/s would need to be computed in the 120-inch model before it could be extended to higher values in the 43.2-inch scale. However, the tail is essentially flat in this region and has been omitted for it and the full-scale beyond 0.7. In contrast, the results reported in Section 4.2, from actual simulations, has each scale extend to an iso-value velocity magnitude of 0.7 m/s in the maximum flow rate, minimum rotation rate case for comparison purposes explained in that section. This extended region was possible because actual FLUENT® edits could be run to provide results at higher values for the 43.2-inch case.

In conclusion, results from the 120-inch scale CFD model can be depicted at the 43.2-inch scale and full-scale with adequate accuracy without actually running the simulators at the other scales. Figure 4-6 through Figure 4-10 showed each of the cases in all scales separated by GPM-RPM pairs.

Table 4-5. Iso-Value Surface Area (scaled) versus Velocity Magnitude (4 pages).

All 120-Inch Runs scaled to Full Scale and 43.2-Inch

Velocity Magnitude (m/s)	120-Inch GPM=98 RPM=0.77 Q3 (sq. m.)	120-Inch GPM=98 RPM=0.48 Q3 (sq. m.)	120-Inch GPM=78 RPM=0.77 Q3 (sq. m.)	120-Inch GPM=78 RPM=0.48 Q3 (sq. m.)	120-Inch GPM=58 RPM=0.77 Q3 (sq. m.)	120-Inch GPM=58 RPM=0.48 Q3 (sq. m.)	43.2-Inch GPM=8.6 RPM=1.51 Q3 (sq. m.)	43.2-Inch GPM=8.6 RPM=0.95 Q3 (sq. m.)	43.2-Inch GPM=6.8 RPM=1.51 Q3 (sq. m.)	43.2-Inch GPM=6.8 RPM=0.95 Q3 (sq. m.)	43.2-Inch GPM=5.2 RPM=1.51 Q3 (sq. m.)	43.2-Inch GPM=5.2 RPM=0.95 Q3 (sq. m.)	Full-Scale GPM=10400 RPM=0.2 Q3 (sq. m.)	Full-Scale GPM=10400 RPM=0.13 Q3 (sq. m.)	Full-Scale GPM=8320 RPM=0.2 Q3 (sq. m.)	Full-Scale GPM=8320 RPM=0.13 Q3 (sq. m.)	Full-Scale GPM=6240 RPM=0.2 Q3 (sq. m.)	Full-Scale GPM=6240 RPM=0.13 Q3 (sq. m.)
0.009							2004.013	2038.907	1619.586	1641.164	1670.774	2059.653							
0.013	2004.013	2038.907	1619.586	1641.164	1670.774	2059.653													
0.018							2100.903	2206.633	1778.515	1827.187	2013.572	2366.600							
0.025													2004.013	2038.907	1619.586	1641.164	1670.774	2059.653	
0.026	2100.903	2206.633	1778.515	1827.187	2013.572	2366.600													
0.027							2272.750	2448.804	2053.820	2081.506	2422.787	2764.850							
0.036							2487.351	2652.104	2379.165	2335.054	2630.955	3050.622							
0.038	2272.750	2448.804	2053.820	2081.506	2422.787	2764.850													
0.045							2731.388	2836.429	2674.941	2525.109	2626.460	3122.695							
0.050													2100.903	2206.633	1778.515	1827.187	2013.572	2366.600	
0.051	2487.351	2652.104	2379.165	2335.054	2630.955	3050.622													
0.055							2936.583	2944.086	2820.650	2615.650	2449.284	2951.571							
0.064							3063.644	2989.847	2823.775	2645.076	2156.496	2636.151							
0.064	2731.388	2836.429	2674.941	2525.109	2626.460	3122.695													
0.073							3100.494	2972.652	2683.372	2588.980	1848.935	2255.114							
0.075													2272.750	2448.804	2053.820	2081.506	2422.787	2764.850	
0.077	2936.583	2944.086	2820.650	2615.650	2449.284	2951.571													
0.082							3075.872	2927.400	2441.879	2459.173	1568.878	1860.724							
0.089	3063.644	2989.847	2823.775	2645.076	2156.496	2636.151													
0.091							2981.890	2819.141	2188.980	2295.268	1318.109	1557.669							
0.100							2845.865	2673.485	1916.307	2114.857	1114.370	1266.278							
0.100													2487.351	2652.104	2379.165	2335.054	2630.955	3050.622	
0.102	3100.494	2972.652	2683.372	2588.980	1848.935	2255.114													
0.109							2664.136	2521.558	1670.593	1928.195	936.676	1015.257							
0.115	3075.872	2927.400	2441.879	2459.173	1568.878	1860.724													
0.118							2449.202	2359.744	1465.906	1740.923	796.247	809.417							
0.125													2731.388	2836.429	2674.941	2525.109	2626.460	3122.695	
0.127							2237.975	2197.827	1289.710	1538.818	673.720	675.476							
0.128	2981.890	2819.141	2188.980	2295.268	1318.109	1557.669													
0.136							2020.330	2019.503	1128.899	1355.902	570.953	573.669							
0.140	2845.865	2673.485	1916.307	2114.857	1114.370	1266.278													
0.145							1816.844	1854.823	983.610	1170.027	493.817	496.397							

Table 4-5. Iso-Value Surface Area (scaled) versus Velocity Magnitude (4 pages).

All 120-Inch Runs scaled to Full Scale and 43.2-Inch

Velocity Magnitude (m/s)	120-Inch GPM=98 RPM=0.77 Q3 (sq. m.)	120-Inch GPM=98 RPM=0.48 Q3 (sq. m.)	120-Inch GPM=78 RPM=0.77 Q3 (sq. m.)	120-Inch GPM=78 RPM=0.48 Q3 (sq. m.)	120-Inch GPM=58 RPM=0.77 Q3 (sq. m.)	120-Inch GPM=58 RPM=0.48 Q3 (sq. m.)	43.2-Inch GPM=8.6 RPM=1.51 Q3 (sq. m.)	43.2-Inch GPM=8.6 RPM=0.95 Q3 (sq. m.)	43.2-Inch GPM=6.8 RPM=1.51 Q3 (sq. m.)	43.2-Inch GPM=6.8 RPM=0.95 Q3 (sq. m.)	43.2-Inch GPM=5.2 RPM=1.51 Q3 (sq. m.)	43.2-Inch GPM=5.2 RPM=0.95 Q3 (sq. m.)	Full-Scale GPM=10400 RPM=0.2 Q3 (sq. m.)	Full-Scale GPM=10400 RPM=0.13 Q3 (sq. m.)	Full-Scale GPM=8320 RPM=0.2 Q3 (sq. m.)	Full-Scale GPM=8320 RPM=0.13 Q3 (sq. m.)	Full-Scale GPM=6240 RPM=0.2 Q3 (sq. m.)	Full-Scale GPM=6240 RPM=0.13 Q3 (sq. m.)
0.150													2936.583	2944.086	2820.650	2615.650	2449.284	2951.571
0.153	2664.136	2521.558	1670.593	1928.195	936.676	1015.257												
0.154							1633.914	1672.361	860.001	1008.154	433.109	428.860						
0.164							1458.616	1512.702	742.865	874.848	387.016	370.252						
0.166	2449.202	2359.744	1465.906	1740.923	796.247	809.417												
0.173							1283.875	1354.235	650.569	767.708	345.527	322.196						
0.175													3063.644	2989.847	2823.775	2645.076	2156.496	2636.151
0.179	2237.975	2197.827	1289.710	1538.818	673.720	675.476												
0.182							1128.435	1203.066	579.446	671.124	301.031	280.167						
0.191							986.651	1065.039	521.642	594.939	261.178	245.049						
0.191	2020.330	2019.503	1128.899	1355.902	570.953	573.669												
0.200							869.717	948.068	470.747	528.521	232.213	217.064						
0.200													3100.494	2972.652	2683.372	2588.980	1848.935	2255.114
0.204	1816.844	1854.823	983.610	1170.027	493.817	496.397												
0.209							773.177	844.274	429.531	468.766	207.934	196.607						
0.217	1633.914	1672.361	860.001	1008.154	433.109	428.860												
0.218							694.436	761.654	385.858	420.260	187.802	180.621						
0.225													3075.872	2927.400	2441.879	2459.173	1568.878	1860.724
0.227							631.182	684.033	346.988	375.032	170.867	167.664						
0.230	1458.616	1512.702	742.865	874.848	387.016	370.252												
0.236							580.066	614.903	311.330	333.813	157.922	155.942						
0.242	1283.875	1354.235	650.569	767.708	345.527	322.196												
0.245							530.691	551.650	278.338	299.190	147.636	146.292						
0.250													2981.890	2819.141	2188.980	2295.268	1318.109	1557.669
0.254							485.329	503.493	252.143	272.296	138.512	137.941						
0.255	1128.435	1203.066	579.446	671.124	301.031	280.167												
0.267							428.055	440.297	223.140	238.310	127.520	127.914						
0.268	986.651	1065.039	521.642	594.939	261.178	245.049												
0.275													2845.865	2673.485	1916.307	2114.857	1114.370	1266.278
0.281	869.717	948.068	470.747	528.521	232.213	217.064												
0.285							363.204	362.658	193.736	205.088	114.268	115.574						
0.294	773.177	844.274	429.531	468.766	207.934	196.607												

Table 4-5. Iso-Value Surface Area (scaled) versus Velocity Magnitude (4 pages).

All 120-Inch Runs scaled to Full Scale and 43.2-Inch

Velocity Magnitude (m/s)	120-Inch GPM=98 RPM=0.77 Q3 (sq. m.)	120-Inch GPM=98 RPM=0.48 Q3 (sq. m.)	120-Inch GPM=78 RPM=0.77 Q3 (sq. m.)	120-Inch GPM=78 RPM=0.48 Q3 (sq. m.)	120-Inch GPM=58 RPM=0.77 Q3 (sq. m.)	120-Inch GPM=58 RPM=0.48 Q3 (sq. m.)	43.2-Inch GPM=8.6 RPM=1.51 Q3 (sq. m.)	43.2-Inch GPM=8.6 RPM=0.95 Q3 (sq. m.)	43.2-Inch GPM=6.8 RPM=1.51 Q3 (sq. m.)	43.2-Inch GPM=6.8 RPM=0.95 Q3 (sq. m.)	43.2-Inch GPM=5.2 RPM=1.51 Q3 (sq. m.)	43.2-Inch GPM=5.2 RPM=0.95 Q3 (sq. m.)	Full-Scale GPM=10400 RPM=0.2 Q3 (sq. m.)	Full-Scale GPM=10400 RPM=0.13 Q3 (sq. m.)	Full-Scale GPM=8320 RPM=0.2 Q3 (sq. m.)	Full-Scale GPM=8320 RPM=0.13 Q3 (sq. m.)	Full-Scale GPM=6240 RPM=0.2 Q3 (sq. m.)	Full-Scale GPM=6240 RPM=0.13 Q3 (sq. m.)
0.300													2664.136	2521.558	1670.593	1928.195	936.676	1015.257
0.303							306.710	304.954	171.889	179.802	103.483	103.489						
0.306	694.436	761.654	385.858	420.260	187.802	180.621												
0.319	631.182	684.033	346.988	375.032	170.867	167.664												
0.320							260.971	261.546	154.877	162.554	93.562	93.445						
0.325													2449.202	2359.744	1465.906	1740.923	796.247	809.417
0.332	580.066	614.903	311.330	333.813	157.922	155.942												
0.338							228.968	228.507	142.017	148.011	84.269	83.841						
0.345	530.691	551.650	278.338	299.190	147.636	146.292												
0.350													2237.975	2197.827	1289.710	1538.818	673.720	675.476
0.356							203.861	203.250	130.797	135.269	76.466	75.232						
0.357	485.329	503.493	252.143	272.296	138.512	137.941												
0.374							183.430	185.603	121.093	124.704	69.650	68.432						
0.375	428.055	440.297	223.140	238.310	127.520	127.914												
0.375													2020.330	2019.503	1128.899	1355.902	570.953	573.669
0.392							168.197	171.403	112.897	115.040	63.869	62.358						
0.400	363.204	362.658	193.736	205.088	114.268	115.574												
0.400													1816.844	1854.823	983.610	1170.027	493.817	496.397
0.409							154.696	159.117	104.915	106.483	58.643	57.634						
0.425	306.710	304.954	171.889	179.802	103.483	103.489												
0.425													1633.914	1672.361	860.001	1008.154	433.109	428.860
0.427							144.657	147.420	96.902	98.925	53.476	52.432						
0.445							134.816	136.989	89.119	92.031	48.633	48.115						
0.450	260.971	261.546	154.877	162.554	93.562	93.445												
0.450													1458.616	1512.702	742.865	874.848	387.016	370.252
0.463							126.654	127.783	82.719	85.536	44.197	44.199						
0.475	228.968	228.507	142.017	148.011	84.269	83.841												
0.475													1283.875	1354.235	650.569	767.708	345.527	322.196
0.481							118.358	119.604	76.235	79.349	40.023	40.529						
0.498							111.157	111.923	70.644	73.814	36.291	37.067						
0.500	203.861	203.250	130.797	135.269	76.466	75.232												
0.500													1128.435	1203.066	579.446	671.124	301.031	280.167

Table 4-5. Iso-Value Surface Area (scaled) versus Velocity Magnitude (4 pages).

All 120-Inch Runs scaled to Full Scale and 43.2-Inch

Velocity Magnitude (m/s)	120-Inch GPM=98 RPM=0.77 Q3 (sq. m.)	120-Inch GPM=98 RPM=0.48 Q3 (sq. m.)	120-Inch GPM=78 RPM=0.77 Q3 (sq. m.)	120-Inch GPM=78 RPM=0.48 Q3 (sq. m.)	120-Inch GPM=58 RPM=0.77 Q3 (sq. m.)	120-Inch GPM=58 RPM=0.48 Q3 (sq. m.)	43.2-Inch GPM=8.6 RPM=1.51 Q3 (sq. m.)	43.2-Inch GPM=8.6 RPM=0.95 Q3 (sq. m.)	43.2-Inch GPM=6.8 RPM=1.51 Q3 (sq. m.)	43.2-Inch GPM=6.8 RPM=0.95 Q3 (sq. m.)	43.2-Inch GPM=5.2 RPM=1.51 Q3 (sq. m.)	43.2-Inch GPM=5.2 RPM=0.95 Q3 (sq. m.)	Full-Scale GPM=10400 RPM=0.2 Q3 (sq. m.)	Full-Scale GPM=10400 RPM=0.13 Q3 (sq. m.)	Full-Scale GPM=8320 RPM=0.2 Q3 (sq. m.)	Full-Scale GPM=8320 RPM=0.13 Q3 (sq. m.)	Full-Scale GPM=6240 RPM=0.2 Q3 (sq. m.)	Full-Scale GPM=6240 RPM=0.13 Q3 (sq. m.)
0.525	183.430	185.603	121.093	124.704	69.650	68.432													
0.525													986.651	1065.039	521.642	594.939	261.178	245.049	
0.550	168.197	171.403	112.897	115.040	63.869	62.358													
0.550													869.717	948.068	470.747	528.521	232.213	217.064	
0.575	154.696	159.117	104.915	106.483	58.643	57.634													
0.575													773.177	844.274	429.531	468.766	207.934	196.607	
0.600	144.657	147.420	96.902	98.925	53.476	52.432													
0.600													694.436	761.654	385.858	420.260	187.802	180.621	
0.625	134.816	136.989	89.119	92.031	48.633	48.115													
0.625													631.182	684.033	346.988	375.032	170.867	167.664	
0.650	126.654	127.783	82.719	85.536	44.197	44.199													
0.650													580.066	614.903	311.330	333.813	157.922	155.942	
0.675	118.358	119.604	76.235	79.349	40.023	40.529													
0.675													530.691	551.650	278.338	299.190	147.636	146.292	
0.700	111.157	111.923	70.644	73.814	36.291	37.067													
0.700													485.329	503.493	252.143	272.296	138.512	137.941	
0.735													428.055	440.297	223.140	238.310	127.520	127.914	
0.784													363.204	362.658	193.736	205.088	114.268	115.574	
0.833													306.710	304.954	171.889	179.802	103.483	103.489	
0.882													260.971	261.546	154.877	162.554	93.562	93.445	
0.931													228.968	228.507	142.017	148.011	84.269	83.841	
0.980													203.861	203.250	130.797	135.269	76.466	75.232	
1.029													183.430	185.603	121.093	124.704	69.650	68.432	
1.077													168.197	171.403	112.897	115.040	63.869	62.358	
1.126													154.696	159.117	104.915	106.483	58.643	57.634	
1.175													144.657	147.420	96.902	98.925	53.476	52.432	
1.224													134.816	136.989	89.119	92.031	48.633	48.115	
1.273													126.654	127.783	82.719	85.536	44.197	44.199	
1.322													118.358	119.604	76.235	79.349	40.023	40.529	
1.371													111.157	111.923	70.644	73.814	36.291	37.067	

Figure 4-11 and Figure 4-12 show all six cases at the same scale, and are the same data in Figure 3-4 scaled to the other scales. Note that the "98 GPM, 0.77 RPM" case will not exactly correspond to the curve in Section 4.2, but matches that discussed in Section 3.0 (depicted in Figure 3-4). The case corresponding to Section 4.2 is shown in Figure 3-4.

The data for these figures comes from Table 4-5 (see Figure 4-5) with the blanks removed since they use consistent velocity-magnitude maps for each individual curve. The velocity-magnitude axis is the one at full-scale or absolute units (unscaled), which is the reason the 43.2-inch curve stops short of 0.7 m/s. The range of particular interest is shaded, and is beyond the peak in each curve.

Since the range of interest shows very different behavior on each of the scales, the solid-fluid interaction may be different on each scale, too. For example, at the 43.2-inch scale the solid could be hurled into the interior by the pump relatively further than at the full-scale (i.e. momentum rather than convection dominated) so that actual experiments at this scale could overstate the ability to move solid at full-scale. Unfortunately, this parameter is one of the time based factors that isn't scaled in favor of equal power per volume, so this effect should be evaluated in light of the final scale-up effort applied to the experiment results in further work.

Figure 4-11. Results from 120-inch Cases Presented in Full-Scale Units.

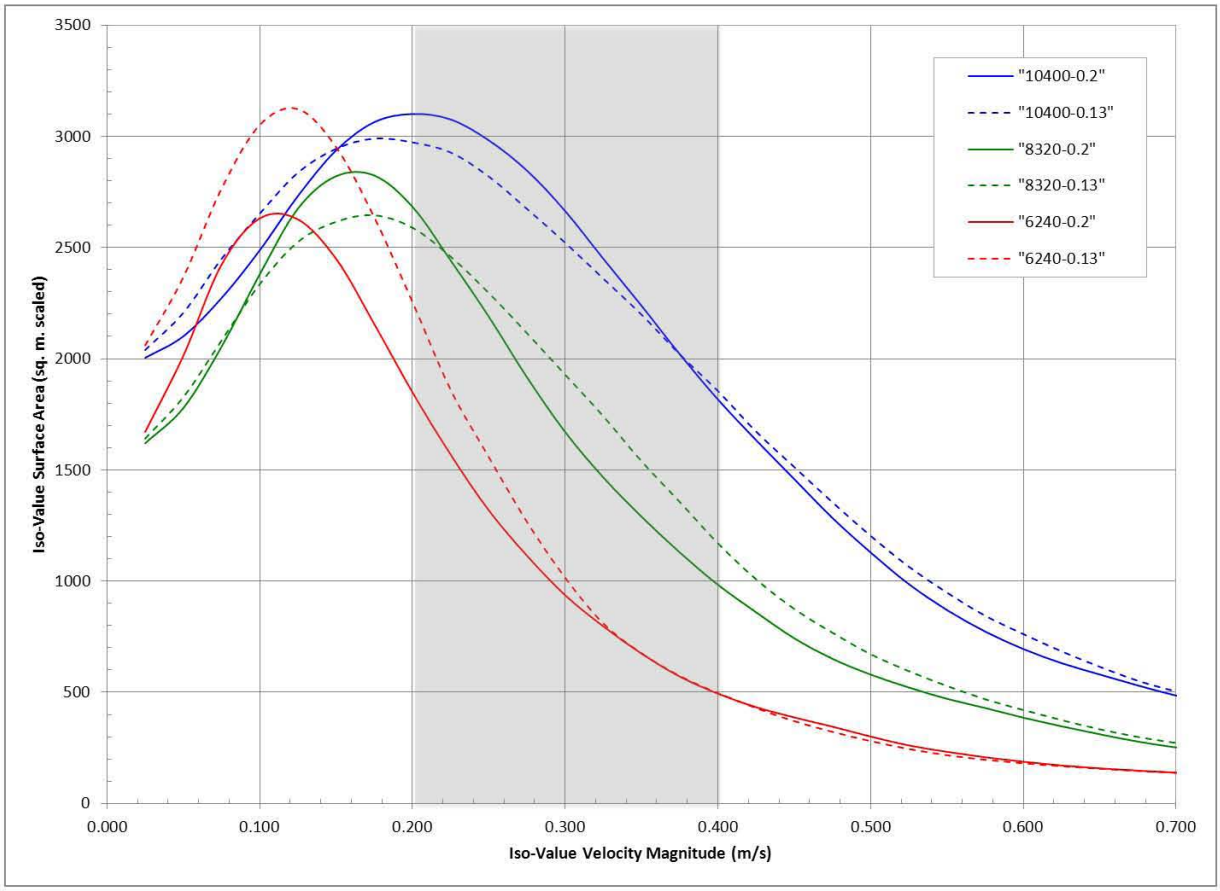

Figure 4-12. Results from 120-inch Cases Presented in 43.2-Inch Units.

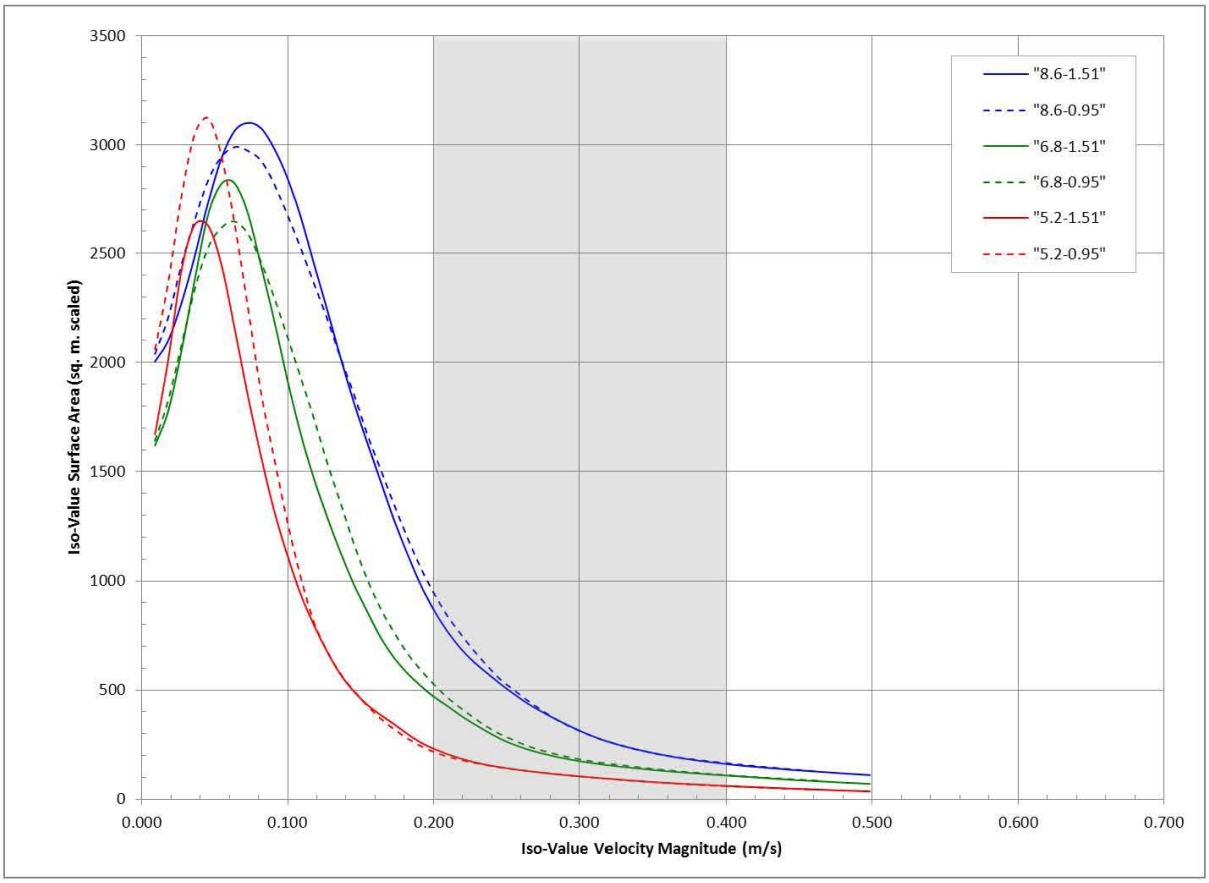

5.0 CONCLUSIONS

The CFD modeling of the DST mixing process that was planned for Tank AY-102 has shown benefit in evaluating various operating scenarios and enhancing the understanding of the mixing impacts. The three major objectives were accomplished. They are listed below along with their outcomes.

1. *Demonstrate that the modeled jet velocities are equivalent to the jet velocities measured in the SSMD 120-inch tank.* Comparisons of the SSMD impellor measurements and the CFD model velocities were sufficient in the region exceeding 20 nozzle diameters, indicating that the CFD fluid parameters match those occurring in the SSMD tanks.

2. *Evaluate the impact of the jet, in terms of its flow rate and rotational rate, on the mixing performance at each of the three scale -- 43.2-inch, 120-inch, and full-scale.* Mixing performance comparisons were developed at all three scales presenting the impacts of changes in flow rate and rotational rate on the mixing performance. At all scales, increasing the flow rate increases the volume of the tank that has an absolute velocity of 0.2 to 0.4 m/s. In some instances, the iso-area increase can be as large as 70%. Rotational rate is a secondary but important factor, especially at the larger scales and the lower flow rates. The large scales and lower flow rates need additional time for the jet to fully penetrate. Therefore the lower rotational rate allows the jet to fully expand and reach further into the tank interior.

3. *Evaluate the correlations that occur between the various scales for a defined particle suspension range of 0.2 to 0.4 m/s, as well as the parameter's impacts on mixing performance.* At each of the three tank scales, the mixing performance in terms of the velocity range of interest (0.2 to 0.4 m/s) was compared. As the tank scale increased, larger portions of the tank had velocity within the range of interest. This result is partly due to the higher jet velocities utilized in the large scales, but does suggest that mixing performance and distribution of solids can be expected to improve as scales get larger. The influence of actual solid particles in these fluid-only simulation streams should be considered when predicting mixing performance.

These results are based upon a sensitivity study of the jet velocity and the rotational rate. These studies have been accomplished using a CFD model that has been tuned to produce jet velocities within the 120-inch tank that compare favorably with the actual jet velocities measured in the 120-inch scale SSMD tank. The same turbulence parameters that were utilized for the 120-inch tank scale have been applied to the 43.2-inch and full-scale CFD tank models.

Using the tuned CFD models, a sensitivity study of the impacts of three jet velocity levels and two rotational rates was performed. Since the CFD model was only analyzing a single fluid model, the results from the 120-inch tank scale could be calculated, with scaling relations used to determine the tank results for the 43.2-inch and full-scale tanks. To confirm the scaling relationships, one CFD model each at 43.2-inch and one at full-scale were generated to compare to the scaled results. These runs compared favorably to the scaled runs, demonstrating an understanding of the scaling relationships for liquid flow between the multiple scales. This understanding has been utilized to scale the 120-inch tank results to the 43.2-inch tank scale and the full-scale to complete the sensitivity matrix.

The fluid-only CFD work is consistent for a range of scaling laws because, locally, the fluid behaves the same in all the models. For example, density or temperature gradients that would

cause the force of gravity to distinguish between scales have been ignored. Thus, the fact that the models are consistent, as demonstrated in Section 4.2, cannot be used to prove that the a-priori choice of one-third power scaling is the correct choice since other assumptions would be just as consistent.

Using the results from the complete sensitivity matrix across all scales, the effects of jet velocity and rotational rate have been studied. In all cases, a change in jet velocity has a much larger impact on mixing than changes in rotational rate. For some of the lower jet velocity cases, the rotation rate can be moderately significant. However, as the jet velocity increases the impact of rotational rate decreases. In terms of the expected key particle movement velocities of 0.2 to 0.4 m/s, the small scale is relatively insensitive to jet velocity. This insensitivity is due to a majority of the tank operating at much lower velocity and the peak iso-areas being well to the left of this velocity range. As the tank scale increases, the iso-area peaks will shift to the right, increasing the mixing impact for a given change in jet velocity. At the full-scale, the iso-area peaks are very near the velocity of interest range of 0.2 to 0.4 m/s, indicating larger changes in mixing performance for a change in jet velocity.

To properly model the solids mixing process, a constitutive model for the solid mixture needs to be combined with the liquid constitutive model used in this study. A constitutive model, in this application, mostly describes momentum transfer between the phases, which ideally should be deduced from experiments at the two physical test stands in the program. Understanding the solid-liquid interaction in sufficient detail will provide confidence in scale-up predictions of the DST mixing process to full-scale using CFD.

6.0 REFERENCES

24590-WTP-ICD-MG-01-019, 2008, *ICD-19 - Interface Control Document for Waste Feed*, Rev. 4, U.S. Department of Energy, Office of River Protection, Richland, Washington.

Abramovich, G. N., 1963, *The Theory of Turbulent Jets*, The MIT Press, Cambridge, Massachusetts.

H-2-34669, *Coil Assembly*, October 1969, Hanford Site Drawing, Richland, Washington.

H-2-34690, *Dome Plan Penetration Tank-102-AY*, March 1971, Hanford Site Drawing, Richland, Washington.

H-2-64447, *Tank Plan and Penetration Schedule*, January 1967, Hanford Site Drawing, Richland, Washington.

Lee, S.Y., R. A. Leishear, R. A. Dimenna, D. B. Stefanko, 2004, "Mixing in Large Scale Tanks - Part I - Flow Modeling of Turbulent Mixing Jets", 2004 ASME Heat Transfer/Fluids Engineering Summer Conference, Charlotte, North Carolina, July 11-15, HT-FED2004-56228.

Lee, S. Y., R. A. Dimenna, R. A. Leishear, D. B. Stefanko, 2008, "Analysis of Turbulent Mixing Jets in a Large Scale Tank", ASME Journal of Fluids Engineering, Volume 130, Number 1,

PL-SSMD-EG-0001, RPP-44650, Rev. 0, 2010, *Waste Feed Delivery Small Scale Mixing Demonstration Plan*, E. Straalsund, Energy Solutions Engineering and Technology, Richland, Washington.

RPP-48055, 2010, *Computational Fluid Dynamics Modeling of Scaled Hanford Double Shell Tank Mixing, Fiscal Year 2010 Model Development Results* (VET-1667-RPT-001), Vista Engineering Technologies, LLC, Richland Washington.

RPP-44619, 2010, *Computational Fluid Dynamics Modeling for Double-Shell Tank Mixing Demonstration Project Work Plan* (VET-1667-PLN-001) Rev. 1, Washington River Protection Solutions, Richland, Washington.

APPENDIX A: PROCESS MOVIE ON CD